WHITE PAPER

JANUARY 2022

PERFORMANCE ANALYSIS OF EVOLUTIONARY HYDROGEN-POWERED AIRCRAFT

Jayant Mukhopadhaya, Ph.D. and Dan Rutherford, Ph.D.

www.theicct.org

communications@theicct.org

twitter @theicct

icct
THE INTERNATIONAL COUNCIL ON CLEAN TRANSPORTATION

BEIJING | BERLIN | SAN FRANCISCO | SÃO PAULO | WASHINGTON

ACKNOWLEDGMENTS

We are grateful to Lahiru Ranasinghe, David Morgan, Oliver Weiß, Fulya Keles, Florian Troeltsch, Andrew Murphy, Valentin Simon, Gniewomir Flis, Stephanie Searle, Yuanrong Zhou, Marie Rajon Bernard, Sola Zheng, Brandon Graver, and Gary Gardner for reviewing an earlier draft. We also thank the Heising-Simons Foundation for their support of this work.

International Council on Clean Transportation
1500 K Street NW, Suite 650
Washington, DC 20005

communications@theicct.org | www.theicct.org | @TheICCT

© 2022 International Council on Clean Transportation

EXECUTIVE SUMMARY

Aviation is a hard-to-decarbonize sector of the transport industry due to the stringent mass and volume requirements for aviation fuel. The high energy content of liquid jet fuel, both per unit mass (specific energy) and per unit volume (energy density), makes it difficult to replace. Significant emphasis has been placed on drop-in Sustainable Aviation Fuels (SAFs) to reduce emissions without sacrificing aircraft performance. But SAFs emit carbon dioxide (CO_2) when combusted (carbon capture during production reduces life-cycle emissions) and their uptake has fallen short of expectations due to their high cost, limited supply, and concerns about the land-use impacts of biofuels.

Interest is growing in hydrogen, particularly liquid hydrogen (LH_2), as a potential alternative to SAFs. LH_2 emits no CO_2 during combustion and can be produced with near-zero carbon emissions if made using renewable electricity ("green hydrogen"). However, its low energy density and heavy cryogenic tank requirements incur performance penalties when compared to Jet A-powered aircraft.

This study explores the potential performance characteristics, fuel-related costs and emissions, and replaceable fossil fuel market of LH_2-powered aircraft entering service in 2035. In keeping with aviation's conservative approach to new aircraft design, only evolutionary advances in design parameters that are feasible by 2035 are considered. Two LH_2 combustion designs are assessed: a smaller turboprop aircraft targeting the regional market, and a narrow-body turbofan aircraft suitable for short and medium-haul flights. These designs are benchmarked against the ATR 72 and the Airbus A320neo, respectively.

Both hydrogen-powered designs will require an elongated fuselage to accommodate LH_2 storage behind the passenger cabin. Gravimetric indices (GI), which denote the ratio of the fuel mass to the mass of the full fuel system including the cryogenic tank, are investigated, at values between 0.2 and 0.35. Seating pitch (SP) values of 29 and 30 inches, mimicking the seating density of low-cost and regular airliners, are used. The potential market coverage of LH_2-powered aircraft families, which include variants of the baseline design with different range and passenger capacities, are analyzed as well.

Overall, we find that LH_2-powered aircraft entering service in 2035 could contribute to aviation's 2050 climate goals but with performance penalties relative to fossil-fuel aircraft. Compared to fossil-fuel aircraft, LH_2-powered aircraft will be heavier, with an increased maximum takeoff mass (MTOM), and less efficient, with a higher energy requirement per revenue-passenger-kilometer (MJ/RPK). They will also have a shorter range than fossil-fuel aircraft. Nevertheless, we estimate that evolutionary LH_2-powered narrow-body aircraft could transport 165 passengers up to 3,400 km and LH_2-powered turboprop aircraft could transport 70 passengers up to 1,400 km. Together, they could service about one-third (31 to 38%) of all passenger aviation traffic, as measured by revenue passenger kilometers (RPKs) (ES 1). This represents 57% to 71% of all RPKs serviced by narrow-body aircraft and 89% to 97% of all RPKs serviced by turboprops. Aircraft with lighter fuel systems (GI of 0.35) and tighter seating density (seating pitch of 29 inches) would provide larger market coverage.

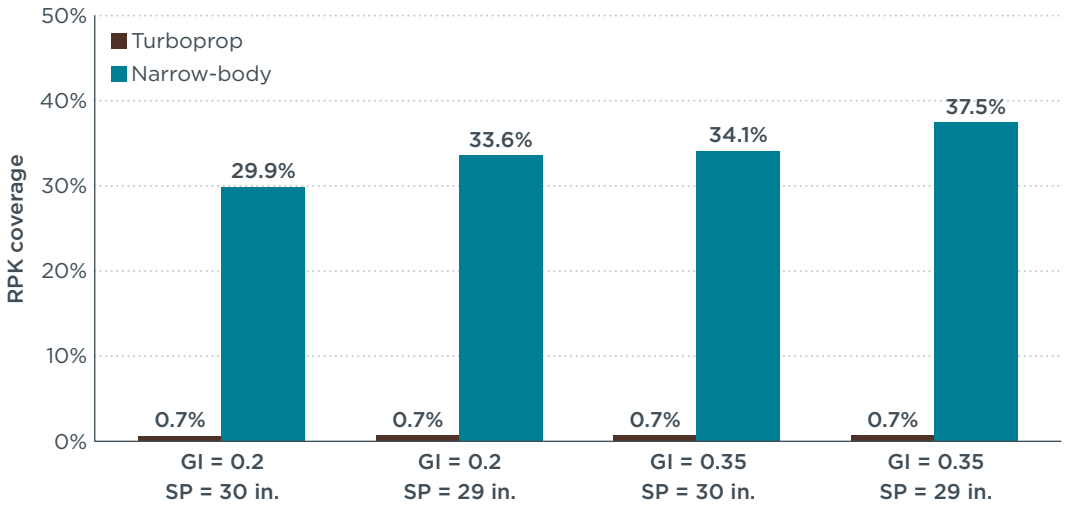

ES 1. Aviation's total RPKs addressable by LH_2-powered aircraft families

Our analysis finds that fuel costs for a green LH_2-powered aircraft will be higher than for Jet A-fueled aircraft, but cheaper than "blue" LH_2 generated from fossil fuels with carbon sequestration or synthetic e-kerosene (ES 2). Taxes levied on CO_2 emissions, represented by the hatched bars, will be needed to make green LH_2 cost-competitive with fossil jet fuel. We estimate that a carbon price of about \$250/tonne-CO_2e would be needed for fuel price parity for LH_2-powered aircraft in the United States in 2035, falling to \$100/tonne-CO_2e in 2050. Europe, where renewable hydrogen is expected to be more expensive, may require a higher CO_2 price to reach cost parity with Jet A. Other benefits from using hydrogen, including reduced air pollution and non-CO_2 climate impacts, are not valued in this calculation.

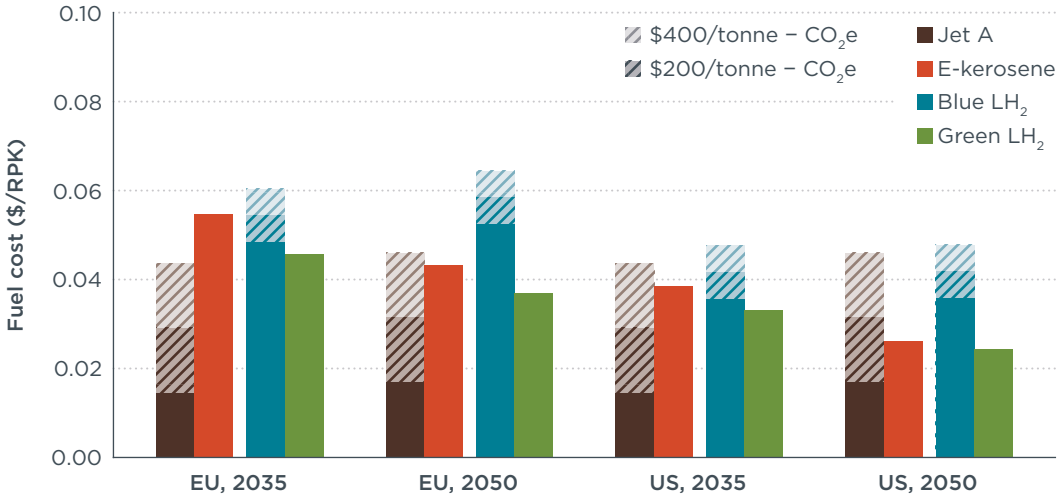

ES 2. Fuel cost by region, 2035 and 2050, with and without carbon pricing

These air-traffic analyses have been carried out with airline route data for 2019. We also project the CO_2e mitigation potential of each LH_2-powered design running on green hydrogen from 2035 to 2050. ES 3 shows the mitigation potential for these aircraft assuming that fleet renewal and growth is sufficient for LH_2 designs to cover between 20% and 40% of the addressable market in 2050. The maximum possible coverage (100%) is also shown in green.

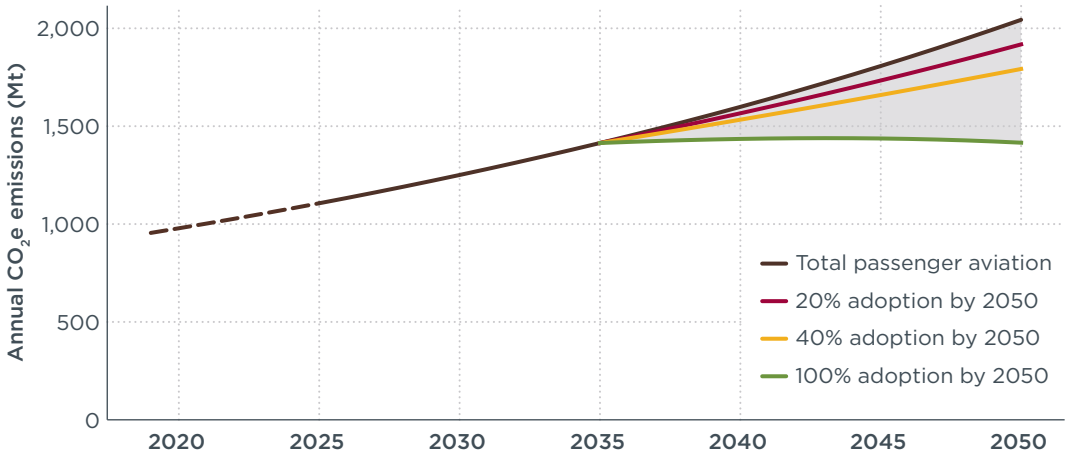

ES 3. CO_2e emissions from passenger aviation under various scenarios of adoption of LH_2-powered aircraft, 2020 to 2050

The 20% to 40% cases yield 126-251 million tonnes (Mt) of CO_2e mitigated in 2050, representing 6-12% of passenger aviation's CO_2e inventory that year. Deployed to their maximum potential (the 100% case), evolutionary LH_2-powered aircraft running on green hydrogen could cap aviation emissions at 2035 levels; other technologies and policies would be needed to further reduce emissions. The 100% cases yield 628 Mt of CO_2e mitigated in 2050, representing 31% of passenger aviation's CO_2e inventory that year.

In summary, while LH_2-powered aircraft do not perform as well as their jet fuel counterparts, they could service one-third of all passenger aviation traffic. Their CO_2e mitigation potential is maximized when fueled by green hydrogen, which is expected to cost more than fossil jet fuel but less than blue hydrogen and e-kerosene. If deployed to their maximum potential, these aircraft could cap aviation emissions at 2035 levels, although a 6-12% reduction in CO_2e emissions, relative to 2050 levels, is more realistic. Finally, to the extent that manufacturers need to prioritize aircraft development, we recommend a focus on narrow-body LH_2 designs since they would provide the highest potential emissions coverage.

TABLE OF CONTENTS

Executive summary ..... **i**

Abbreviations ..... **vi**

Introduction **1**

Methods **4**

Reference aircraft 4

Aircraft modeling 4

Fuel analysis 8

Results **11**

Aircraft design 11

Reference mission simulations 13

Addressable market 17

Hydrogen production requirements 21

CO_2 mitigation potential 22

Conclusions **24**

Bibliography **26**

Appendix A: Hydrogen storage **29**

Appendix B: Aircraft mission profile **31**

LIST OF FIGURES

ES 1. Aviation's total RPKs addressable by LH_2-powered aircraft families ii

ES 2. Fuel cost by region, 2035 and 2050, with and without carbon pricing ii

ES 3. CO_2e emissions from passenger aviation under various scenarios of adoption of LH_2-powered aircraft, 2020 to 2050 iii

Figure 1. Carbon intensity of fuels investigated 9

Figure 2. Fuel price by region, 2035 and 2050. 10

Figure 3. Representation of the tank and passenger cabin layout for the LH_2-powered turboprop 12

Figure 4. Representation of the tank and passenger cabin layout for the LH_2-powered narrow-body 13

Figure 5. Narrow-body aircraft carbon intensity by fuel type, GI = 0.275 16

Figure 6. Fuel cost by region, 2035 and 2050, with and without carbon pricing. 16

Figure 7. 2019 turboprop missions compared to the payload-range capability of LH_2-powered turboprop (GI = 0.275, SP = 30 in.) 18

Figure 8. Percentage of turboprop RPKs covered by LH_2-powered aircraft 19

Figure 9. 2019 narrow-body missions compared to the payload-range capability of an LH_2-powered narrow-body (GI = 0.275, SP = 30 in.) 20

Figure 10. Percentage of narrow-body RPKs covered by LH_2-powered aircraft 20

Figure 11. Total RPK coverage of LH_2 aircraft families by aircraft class, GI, and seat pitch 21

Figure 12. Demand projection for green LH_2 assuming different aircraft adoption rates 22

Figure 13. CO_2e emissions from passenger aviation under various scenarios of adoption of LH_2-powered aircraft, 2020 to 2050 23

Figure A1. Turboprop RPK coverage and MTOM as a function of the LH_2 fuel system's gravimetric index. 30

Figure A2. Narrow-body RPK coverage and MTOM as a function of the LH_2 fuel system's gravimetric index. 30

LIST OF TABLES

Table 1. Thermodynamic properties of Jet A, e-Kerosene, GH_2, and LH_2 2

Table 2. Hydrogen storage in automobile and spacecraft applications 6

Table 3. LH_2 aircraft design parameters 11

Table 4. Weights, range, and fuel intensity of the turboprop aircraft 14

Table 5. Weights, range, and fuel intensity of the narrow-body aircraft 14

Table 6. Energy and emissions intensity of the turboprop aircraft 15

Table 7. Energy and emissions intensity of the narrow-body turbofan aircraft 15

Table A1. Liquid hydrogen storage properties 29

ABBREVIATIONS

AR	aspect ratio
BWB	blended wing body
CCS	carbon capture and sequestration
CO_2	carbon dioxide
DAC	direct air capture
EIS	entry into service
GH_2	gaseous hydrogen
GI	gravimetric index
H_2	hydrogen
ICAO	International Civil Aviation Organization
ICCT	International Council on Clean Transportation
L_{cabin}	length of passenger cabin
L_{galley}	length of the galley
L_{tank}	length of the liquid hydrogen tank
LCA	life cycle analysis
LH_2	liquid hydrogen
MF	mass fraction
η_f	maximum allowable fill percentage of LH_2 tank
MTOM	maximum takeoff mass
Mt-CO_2e/year	million tonnes of CO_2 equivalent emissions per year
OEW	operating empty weight
PAX	passengers
η_V	percentage of fuselage volume available for LH_2 storage
R_{fuse}	radius of the fuselage
RPK	revenue passenger kilometer
S_P	seat pitch: distance between two rows of seats
S_A	seats abreast: number of seats in a row
SAF	sustainable aviation fuel
SMR	steam methane reforming
STP	standard temperature and pressure
Taper ratio	ratio of the root and tip chord lengths of the wing
V_{LH_2}	volume of liquid hydrogen

INTRODUCTION

Aircraft emit significant amounts of climate pollution. In 2019, commercial airlines emitted more than 900 million tonnes of carbon dioxide (CO_2) (Graver et al., 2020); treated as a country, global aviation would be the sixth largest source of CO_2, roughly equal to the emissions of the German and Dutch economies combined (European Commission, 2020). CO_2 emissions from aircraft are expected to roughly double by mid-century (International Air Transport Association (IATA), 2020); and the total (CO_2 + non-CO_2) climate impact of flying could be three times that of CO_2 alone (Lee et al., 2021). Further efforts are needed if aviation is to contribute its fair share to climate protection under the Paris Agreement.

In the near-term, improvements in fuel efficiency due to fleet turnover and improved operations will reduce emissions more than fuel switching. That being said, prior to the COVID-19 downturn, traffic, in terms of revenue passenger kilometers (RPKs)[1] traveled, was increasing four times faster than fuel efficiency was improving (Graver et al., 2020). Even worse, from 2005 to 2019, almost all growth in CO_2 emissions (90%) in the United States came from more fuel-efficient low-cost carriers, which outgrew their fuel efficiency improvements even faster than network carriers (Graver & Rutherford, 2021). While important, fuel efficiency alone will not be enough for airlines to meet their climate protection goals.

Thus, the heavy lifting in reducing the climate impact of aviation will need to come from fuel switching. To date, most industry interest has focused on the development of Sustainable Aviation Fuels (SAFs). Still, progress has been slow due to limited supply, high cost, and concerns about the land-use impacts of first-generation biofuels produced from crops. Early voluntary aviation targets have been widely missed (e.g., 6% by 2020, see (Air Transport Action Group (ATAG), 2011) with SAF only accounting for about 0.05% of global jet fuel use today (International Air Transport Association (IATA), 2021; Mikosz, 2021).[2] The advantages of SAFs are clear—as drop-in fuels, they can be used in up to 50% blends in existing aircraft, and they have sufficient energy per unit volume (energy density) to fuel even long-haul flights. But they still emit CO_2 when burned.

While the slow pace of SAF development has led governments to propose mandating SAF use (European Commission, 2021b) and subsidizing it (Brownley, 2021), industry is also starting to explore alternative propulsion technologies. Turboelectric concepts combine the higher efficiency of electric propulsion systems that can be distributed or integrated into the fuselage with a hydrocarbon burning turbine to provide 7-12% reductions in fuel burn (Welstead & Felder, n.d.). More recently, Embraer announced a 9-passenger parallel hybrid-electric propulsion aircraft set to fly by 2030 that claims to reduce CO_2 emissions by 50% (Embraer, 2021). But the emissions reduction impact of a 9-passenger aircraft with a range of 500 nautical miles (925 km) is small.

The continued use of fossil jet fuel ("Jet A") does not reduce the CO_2 and non-CO_2 impact per unit of fuel, helping explain the interest in pure battery electric aircraft. Small all-electric aircraft such as Eviation's Alice (*Aircraft – Eviation*, n.d.) and Heart Aerospace's ES-19 (*Heart Aerospace | Electrifying Regional Air Travel*, n.d.) provide truly zero-emission aviation, but the limitations in battery energy per unit mass (specific energy) severely limit the aircraft's range and, therefore, the potential market share of those aircraft.

Hydrogen has been touted as a promising alternate energy source due to its high energy content per unit mass (specific energy) and because a clear pathway to zero-

1 RPK = number of passengers x distance traveled

2 100 million liters of SAF production in 2021 compared to an estimated 215 billion liters of jet fuel usage in the same year. This means that SAFs accounted for 0.047% of global jet fuel use.

emission production exists, using entirely renewable electricity ("green hydrogen"). Both internal combustion and fuel cell aircraft are being explored. Fuel cell technology has been rapidly improving. Partnerships between ZeroAvia and Alaska Air Group (ZeroAvia | Alaska Air Group | Hydrogen Powertrain, 2021) promise to bring fuel-cell powered aircraft to the regional market with a retrofitted 76-seat aircraft. The regional segment accounted for 7% of passenger aviation's total CO_2 emissions in 2019 (Graver et al., 2020).

In September 2020, Airbus announced its ZEROe initiative to develop hydrogen-powered commercial aircraft that could enter service in 2035 (Airbus, 2020). This timeline gives them five years to design, test, and mature the required technologies, two years to finance and organize supply chains, and eight years to manufacture and bring the aircraft to market. Three concepts were unveiled. Two concepts followed the conventional tube-and-wing configuration which represent evolutionary progress in aircraft designs, and one followed the blended-wing body (BWB) configuration which represents a revolutionary change in aircraft design.

A significant challenge for hydrogen-powered aircraft design is fuel storage. Jet A is simple to store in integral tanks within the wing structure, with additional fuel stored in fuselage tanks.[3] Hydrogen stores 2.8 times the energy on a per unit mass basis than Jet A. However, its volumetric energy density is significantly lower than that of Jet A. At standard temperature and pressure (STP), defined as 0°C at 100 kPa, hydrogen is a gas with a density of 0.899 kg/m^3 (Makridis, 2016). Jet A, with its density of 808 kg/m^3 (Chevron, 2007), is ~900 times as dense. For sufficient hydrogen to be carried in an aircraft, its density needs to be increased. This is achieved by storing gaseous hydrogen (GH_2) at high pressure, or by liquefying it and storing the liquid hydrogen (LH_2) at very low temperatures.

The industrial standard is to store GH_2 at 700 MPa (700 bar or ~700x atmospheric pressure) and at ambient temperature. Higher pressure storage is possible, but with diminishing gains in energy density. Hydrogen has a boiling point of -253°C (20 K) at atmospheric pressure. Current solutions store LH_2 at slightly above atmospheric pressure (1.01-1.5 bar or 101-150kPa) at cryogenic temperatures of -253 to -248°C (20-25 K).

Table 1 lists the energy and density characteristics of the fuels at these storage conditions. The main takeaway is that producing the energy of a unit volume of Jet A requires 7 times that volume of compressed GH_2 and 4 times that volume of LH_2. This makes LH_2 the superior option from the perspective of improving the payload capacity and range of potential aircraft designs.

Table 1. Thermodynamic properties of Jet A, e-Kerosene, GH_2, and LH_2

	Jet A	E-kerosene	Compressed gaseous H_2	Liquid H_2
Specific energy (MJ/kg)	43	43 (1x)	120[4] (~2.8x)	
Density (kg/m^3)	808	808 (1x)	42 (~0.05x)	71 (~0.09x)
Energy density (GJ/m^3)	34.7	34.7 (1x)	5 (~0.14x)	8.5 (~0.25x)

LH_2-powered aircraft will be most impactful if they can replace regional and especially narrow-body aircraft like Airbus's A320 and Boeing's 737 MAX families powered by

3 The word integral indicates that these tanks are part of the aircraft structure itself with fuel being stored between sealed structural elements such as the ribs and skin of the wing. These tanks do not need any pressurization or temperature control.

4 The Lower Heating Value (LHV) of hydrogen is used here, as the product of hydrogen combustion would be water vapor.

fossil fuels. These narrow-body aircraft accounted for more than half of passenger aviation's total CO_2 emissions in 2019 (Graver et al., 2020), and aren't suitable for electrification for the foreseeable future.

The Cryoplane project (Westenberger, 2003) remains the most detailed technical study of hydrogen-powered aircraft and the technological challenges associated with their development. Its sub-system level analysis did not uncover insurmountable technical challenges to the development of these aircraft, but the study did not address the potential market or climate impact of these aircraft. More recent analysis of the technology, economics, and climate impact of hydrogen aviation (McKinsey & Company, 2020) suggests a variety of potential aircraft could be developed, from fuel-cell powered models for commuter and regional segments, to hybrid hydrogen-powered ones for short- to long-haul segments, each with different time horizons for entry into service (EIS). It does not provide detailed design analysis or a quantification of the addressable market of these designs.

This study fills the gap and evaluates the performance of LH_2-combustion aircraft that could enter service in 2035. Two designs are assessed: a smaller turboprop aircraft for regional flights, and a narrow-body turbofan aircraft for short- and some medium-haul operations. By performance, we refer to the payload-range capability, fuel-related emissions and costs, and potential market size of those designs. In keeping with aviation's conservative approach to new aircraft design, only evolutionary advances in design parameters that are feasible in the 2035 timeframe are considered. Aircraft technology is frozen to currently available levels and the only advances considered are the development of hydrogen combustion propulsion systems and LH_2 storage solutions. In contrast, we use best-case scenarios for the carbon intensity of the alternative fuels considered in this study to quantify the maximum possible impact of the LH_2-powered aircraft.

The focus of this work is aircraft performance and the resulting market; accordingly, other issues that will help determine the viability of hydrogen as an aviation fuel are not addressed. We do not consider the infrastructure requirements or the safety concerns surrounding the production, delivery, and storage of hydrogen. Revolutionary changes to aircraft design, such as blended-wing body (BWB) aircraft, are not explored as these are unlikely to enter production by 2035. Propulsion concepts such as hybrid-electric propulsion, distributed propulsion, and open-rotor designs are excluded for the same reason. Fuel cells and gaseous hydrogen storage are not addressed in this study either. It is assumed that hydrogen-combustion propulsion systems can be developed in this timeframe.[5] Freight is not analyzed in this study. Finally, the impact of contrail/cirrus formation, and NO_x and soot emissions of the different fuels, are not considered.

The rest of this paper is arranged as follows. The next section outlines the methods we used to assess these aircraft. We then present our main results, including the expected LH_2 aircraft performance characteristics; the fuel costs and the life-cycle analyses associated with using Jet A, e-kerosene, green LH_2, and blue LH_2; and the share of RPKs and passenger CO_2 that could be mitigated by LH_2-powered aircraft. We close with some policy recommendations and thoughts on future work.

5 This will require significant investment in research and development as a clean-sheet design of the engine is required. Some key technical challenges that need to be addressed: component wear due to hydrogen embrittlement and higher combustion temperatures, handling the higher flame speed of hydrogen, and new combustion control mechanisms with new fuel injectors. In addition to monetary investment, the experimental development of new engines will require additional time to budget for potential prototype failures, fatigue testing, and engine certification.

METHODS

The following sections outline our research methods. First, we present the reference aircraft and the target performance metrics used to assess the hydrogen-powered aircraft designs. Next, we describe how we estimated the payload, range, and energy efficiency of each design. Finally, we outline the calculation of the lifecycle emissions and cost of fueling conventional aircraft with Jet A and e-kerosene, and hydrogen-powered aircraft with blue and green LH_2.

REFERENCE AIRCRAFT

In this study, we focus on evolutionary tube-and-wing designs as these are more likely to enter the market by 2035. Aviation's focus on safety makes revolutionary re-designs difficult. Since a hydrogen-powered propulsion system is already a significant technological change, bringing it to market on a BWB configuration, which has no precedent in commercial aviation, is unlikely in the near- to mid-term. In a similar evolutionary vein, only hydrogen combustion is considered for the propulsion system. Existing turbine designs can run on hydrogen with a few modifications, as suggested by the Cryoplane project (Westenberger, 2003).

In this study, we developed reference aircraft using the two evolutionary liquid hydrogen designs investigated under Airbus's ZEROe program. The hydrogen-powered aircraft put forward by Airbus are still in the conceptual design stage with no firm geometrical or performance parameters. Airbus provides target payload and range numbers that were used to select existing Jet A-powered reference aircraft. Those were subsequently modified to accommodate the LH_2 storage system. The reference aircraft's representative missions were also used to estimate the addressable market of LH_2-powered designs.

The smaller aircraft, powered by two turboprop engines, is expected to carry fewer than 100 passengers over ranges greater than 1,000 nautical miles (1,850 km). The chosen reference turboprop aircraft is the ATR 72-600 which has a stated range of 1,404 km with 78 passengers (ATR, 2020). The larger aircraft, powered by two turbofan engines, is expected to carry fewer than 200 passengers over ranges greater than 2,000 nautical miles (3700 km). The chosen reference narrow-body turbofan aircraft is the Airbus A320neo which can carry 165 passengers over 6,500 km (Airbus, n.d.). The reference aircraft are used as starting points for the design of the hydrogen-powered aircraft.

AIRCRAFT MODELING

Geometry

Keeping with the theme of evolutionary design, the LH_2-powered aircraft designs rely heavily on current in-service aircraft. An operational constraint for the aircraft design is its takeoff field length (TOFL) and wingspan, imposed by the need to stay within the same ICAO Aerodrome reference code as the reference aircraft (International Civil Aviation Organization (ICAO) et al., 2016). This ensures that the LH_2-powered aircraft can operate out of the same airports as their reference counterparts.

For the turboprop this limits the TOFL to less than 1,800 m and the wingspan to less than 36 m. For the narrow-body, this limits the wingspan to less than 36 m but there isn't a strict limit for the TOFL. The wingspan constraints are directly applied in the vehicle modeling, whereas the TOFL of the reference aircraft is retained by keeping the wing loading and takeoff thrust-to-maximum takeoff mass (MTOM) ratio identical to that of the reference aircraft (Scholz, n.d.). Wing loading is defined as the ratio of the aircraft's MTOM to the surface area of its main wing. It affects the aircraft's takeoff and landing distances, its maneuverability, and stall speeds. Keeping the wing loading

identical to the reference aircraft ensures that the new aircraft is certifiable without carrying out detailed flight simulations. For example, if the MTOM of the LH_2-powered aircraft is higher, its wing area will also have to increase, and vice versa.

Fuselage

For the fuselage, the diameter, nose length, and tail length are kept identical to the reference aircraft. The fuselage is elongated to accommodate the LH_2 tank while maintaining passenger capacity for the base design. The LH_2 storage is assumed to be a single cylindrical tank behind the rear bulkhead of the passenger cabin. The length of the fuselage is increased in a one-to-one proportion to the length of the fuel tank.

The length of the passenger cabin is calculated as:

$$L_{cabin} = S_P \left\lceil \frac{PAX}{S_A} \right\rceil + L_{galley} \qquad (1)$$

where L_{galley} is the length of the galley (4.3 m for turboprop, 6 m for narrow-body), PAX is the number of passengers, S_A is the number of seats abreast (4 for turboprop, 6 for narrow-body), and S_p is the seating pitch (0.737 and 0.765 m or 29 and 30 inches). The seating pitch is the distance between two consecutive rows of seats, measured at the same point on each seat. The $\lceil\ \rceil$ operator rounds up to give an integer number of rows. The total length of the fuselage is a simple sum of the lengths of the nose, cabin, LH_2 tank, and tail.

To ensure operational feasibility without significant higher-fidelity analyses to rule out design constraints, such as tail strike during takeoff, the maximum fuselage length is limited to a similar, certified, in-service aircraft. In the case of the turboprop, the fuselage length is limited to that of the De Havilland Canada Dash 8-Q400 which has the largest passenger capacity of any current turboprop. In the case of the narrow-body, the fuselage length is limited to that of the Airbus A321neo, the longest variant of the A320neo family.

Wing

For wing design, the design variables that were explored are wingspan, aspect ratio, and taper ratio.[6] Parameter sweeps in these variables are used to determine the optimal values. No significant changes are made to the wing design of the narrow-body as the A320neo has a recently designed wing that cannot be improved without high-fidelity analysis. Additionally, the wing is at the limit (36 m) of the wingspan that keeps it in the C category of the ICAO Aerodrome reference code.

More significant changes were made to the ATR 72 wing as this is an older aircraft (1989 EIS) that hasn't been redesigned with newer aviation technologies. There is also more freedom as the ATR 72 wingspan is 27 m, compared to the 36 m limit for the C category. Parameter sweeps in the wingspan, aspect ratio, and taper lead to a larger wingspan, higher aspect ratio and a more tapered wing (lower taper ratio) to increase the aircraft's fuel efficiency. The horizontal and vertical stabilizers are scaled proportional to the change in the surface area of the main wing.

Hydrogen Storage

While the mass of hydrogen required to provide an equivalent amount of energy is approximately one-third the mass of Jet A needed, the pressurization requirement for GH_2 and the cryogenic requirement for LH_2 result in heavy storage tanks. The parameter commonly used to quantify the storage efficiency of a fuel tank is its mass

6 The aspect ratio of a wing is defined as the ratio of its span to its mean chord. A high aspect ratio indicates to a long narrow wing. The taper ratio of a wing is defined as the ratio of its tip chord to its root chord. A high taper ratio indicates a wing that is significantly narrower at its tip than at its root.

fraction (MF), defined as the mass of fuel divided by the mass of the tank system including the fuel.

In addition to the heavier fuel tank, LH_2-powered aircraft will require a modified fuel delivery system which includes a heat exchanger to convert LH_2 to GH_2 before combustion, and redesigned fuel pipes, pumps, seals, and valves to handle the increased volumetric flow and the cryogenic temperatures. In the absence of a rigorous method to calculate the weight of these systems, their weight is lumped together with the mass of the tank as the Gravimetric Index (GI) of the fuel system. This is defined as

$$GI = \frac{Mass\ of\ stored\ fuel}{Mass\ of\ stored\ fuel + Mass\ of\ the\ entire\ fuel\ system} \qquad (2)$$

where the fuel system refers to the empty weight of the storage tanks, any required heat exchangers, and all other ancillary fuel delivery components such as pipes, pumps, valves, and sealants. Consequently, the GI of a fuel system will always be less than or equal to the MF of the fuel tank.

Jet A can achieve very high mass fractions (essentially 1.0) with integral fuel tanks that are built into the structure of the wing. To achieve specific energy parity between hydrogen and Jet A at a system level, a GI of 0.34 would be required for the hydrogen fuel system. Table 2 presents the mass fractions of existing hydrogen storage solutions, which increase as the mass of the stored hydrogen grows. There is a large gap in data for tanks that store 1,000–5,000 kg of hydrogen, which is the requisite amount for regional to short-haul aircraft.

Table 2. Hydrogen storage in automobile and spacecraft applications

	Mass of hydrogen stored (kg)	Fuel tank mass fraction
Toyota Mirai GH_2 storage	5	0.06
Shuttle on-board LH_2 storage	100	0.25
Ariane fuel tank (LH_2)	28,000	0.84
Shuttle external tank (LH_2)	230,000	0.83

While structural and thermal analysis suggests that a fuel tank MF of 0.5–0.8 (Gomez & Smith, 2019; Verstraete, 2009) can be achieved for LH_2, this work assumes GI in the range of 0.2–0.35 for the fuel system. This approach is conservative but matches the time frame (2035) and scope (evolutionary, rather than revolutionary designs). This may overestimate the mass penalty for LH_2, translating to a lower efficiency, shorter maximum range, and higher maximum takeoff mass (MTOM)[7] than what might be achievable in the long-term.

Further information about hydrogen storage and the sensitivity of our results to GI assumptions is provided in Appendix A: Hydrogen storage.

Weight estimation

Original equipment manufacturer (OEM)-provided weights are used when modeling the reference aircraft. The National Aeronautics and Space Administration's (NASA) Flight Optimization System weight estimation method (Wells et al., 2017) is used to estimate the weights for the hydrogen-powered aircraft. The weight estimation module (WEM) was validated by comparing the OEM-provided weights for the reference aircraft to those predicted by the module. It overestimated the Operating Empty

7 Maximum takeoff mass denotes the maximum sum of aircraft empty weight, payload, and fuel that an aircraft is certified to operate at. It corresponds to Gross Vehicle Weight for road vehicles.

Weight (OEW) of the ATR 72 by 235 kg (+1.7%) and underestimated the OEW of the A320neo by 325 kg (-0.8%).

For the payload weight estimation, the module assumes a passenger weight of 74.8 kg (165 lbs). The baggage weight varies based on the range of the aircraft. Baggage weights of 20.0 kg (44 lbs) and 15.9 kg (35 lbs) are used for the narrow-body and turboprop aircraft, respectively.

The WEM uses an initial guess for the aircraft's MTOM as a starting point to estimate the weights of the structural components. The output MTOM can be different from the input value. This necessitates a feedback loop to ensure the output MTOM is identical to the input MTOM. The MTOM for the LH_2-powered aircraft represents the weight of the aircraft at maximum fuel and payload capacity.

Sizing

The reference aircrafts' MTOM, engine weight, engine thrust, and lifting surface areas are used as baselines for the corresponding LH_2-powered aircraft. The main wing's area and the engine thrust are scaled proportional to the estimated MTOM of the LH_2-powered aircraft such that the wing loading and the thrust-to-MTOM ratio of the aircraft remains the same. The horizontal and vertical stabilizers are sized to keep the tail volume coefficient constant.[8] The sizing is done within the weight estimation loop so that the effects of the changing geometry and components are included in the final MTOM estimation.

Performance

Once the aircraft has been correctly sized and its weight estimated, its aerodynamic performance is analyzed. The aircraft analysis and mission simulation is carried out using SUAVE, an open-source simulation environment built for conceptual vehicle design and optimization (Botero et al., 2016; Lukaczyk et al., 2015). A low-fidelity aerodynamic analysis is performed to rapidly calculate the lift and drag characteristics of the aircraft. This is known as the *Fidelity Zero* analysis (Lukaczyk et al., 2015).

For the propulsion systems, the turboprop engine performance characteristics are taken from Piano 5.[9] The specific fuel consumption is kept identical between the jet fuel- and hydrogen-powered turboprops on an energy equivalent basis (J/s-N). The turbofan is modeled within SUAVE as a Gas-Turbine energy network according to specifications of the Pratt & Whitney PW1100G engine[10] that powers the A320neo. The LH_2-powered turbofan is scaled to keep the thrust-to-MTOM ratio identical to that of the A320neo. The mission profile used to assess the energy intensity of the hydrogen-powered designs is provided in Appendix B: Aircraft mission profile. Fuel reserves are included in all calculations.

Aircraft families

It is common practice for aircraft OEMs to create aircraft families, where the same wing is attached to fuselages of varying length to cater to airlines that might have different payload needs. The reference aircraft are themselves part of product families. The ATR 72 has a smaller 48-seat variant in the ATR 42. The A320neo is part of a family that includes a 140-seat variant in the A319neo, and a 206-seat variant in the A321neo. Similarly, we simulate LH_2-powered aircraft families where the fuselage and wing are held constant, but passenger capacity and tank size are traded to either increase

8 The tail volume coefficient is a design metric that influences the aircraft's static stability characteristics (MIT OCW, 2006). Keeping it identical to the reference aircraft ensures the horizontal and vertical stabilizers are sized correctly to provide enough control authority to the aircraft. A bigger tail empennage is needed for LH_2-powered aircraft as their center-of-gravity is shifted towards the back due to the placement of fuel tank behind the passenger cabin.

9 https://www.lissys.uk/Piano5.html

10 https://prattwhitney.com/products-and-services/products/commercial-engines/pratt-and-whitney-gtf

range at a lower passenger capacity or increase passenger capacity at the expense of maximum range.

For the turboprop, 50-, 70-, and 78-seat variants are investigated and are considered one aircraft family. In creating these variations, the maximum fuselage length constraint is joined by a constraint on the length of the LH_2 tank (see Appendix A for discussion on tank geometry). The length of the LH_2 tank is limited to 3.5 m to keep the increase in MTOM relative to the ATR 72 to less than 25%. The tank length constraint is active for the 50- and 70-seat aircraft and, as a consequence, the fuselage length is less than the Dash8-400 (< 32.8 m). For the 78-seat aircraft, the fuselage length constraint is active, and the tank length is limited to 2.76 to 3.17 m, depending on the assumed seat pitch in the passenger cabin. The wing and tail for the aircraft family is sized based on the 70-passenger variant and is kept the same across all the variants.

For the narrow-body, 140-, 150-, 168-, 192-, and 200-seat variants are investigated. The three-aircraft combination that provides the best RPK coverage is considered the aircraft family. In this case, the fuselage length is kept identical to the A321neo for all variants and the passenger capacity is directly traded for fuel storage capacity. The wing and tail for the narrow-body family is sized based on the 168-passenger variant and is also kept identical across the different variants.

FUEL ANALYSIS

For this study we consider four different fuels: traditional Jet A aviation fuel and synthetic "e-kerosene" that would fuel conventional hydrocarbon-powered aircraft, and blue and green LH_2 that would fuel the hydrogen-powered designs. "E-kerosene" is a synthetic jet fuel that can be used in existing aircraft engines as a drop-in replacement to Jet A. If produced using additional renewable electricity and carbon captured either as a waste from a point source or using direct air capture (DAC), e-kerosene can be a near-zero emission aviation fuel.

Two production pathways for hydrogen were considered. Blue hydrogen denotes hydrogen produced using natural gas steam methane reforming (SMR) but with a share of the resulting CO_2 captured via carbon capture and sequestration (CCS). Life-cycle emissions from blue hydrogen are sensitive to assumptions of methane leakage and carbon capture rates (Zhou et al., 2021). Green hydrogen is defined as being produced by 100% additional renewable energy.

For all the fuels considered, the life-cycle emission calculations are consistent with the Carbon Offsetting and Reduction Scheme for International Aviation's (CORSIA) methodology (International Civil Aviation Organization (ICAO), 2020).[11] The carbon intensity calculations use the 100-year global warming potentials of CH_4 and N_2O to convert them into CO_2-equivalent units (Intergovernmental Panel on Climate Change (IPCC), 2014). We do not estimate the warming impact of short-lived climate pollutants like NO_x, black carbon, water vapor, or contrail cirrus. For all fuels, we do not include the carbon intensity of building the infrastructure for fuel production. For the alternative fuels we assume the best-case scenarios for their well-to-wake life-cycle emissions to quantify their maximum mitigation potential.

11 CORSIA is a United Nations policy under which airlines are required to offset most growth in international emissions after 2019. Life cycle assessment methods and default emission values by fuel type were generated to reward the use of SAFs under CORSIA.

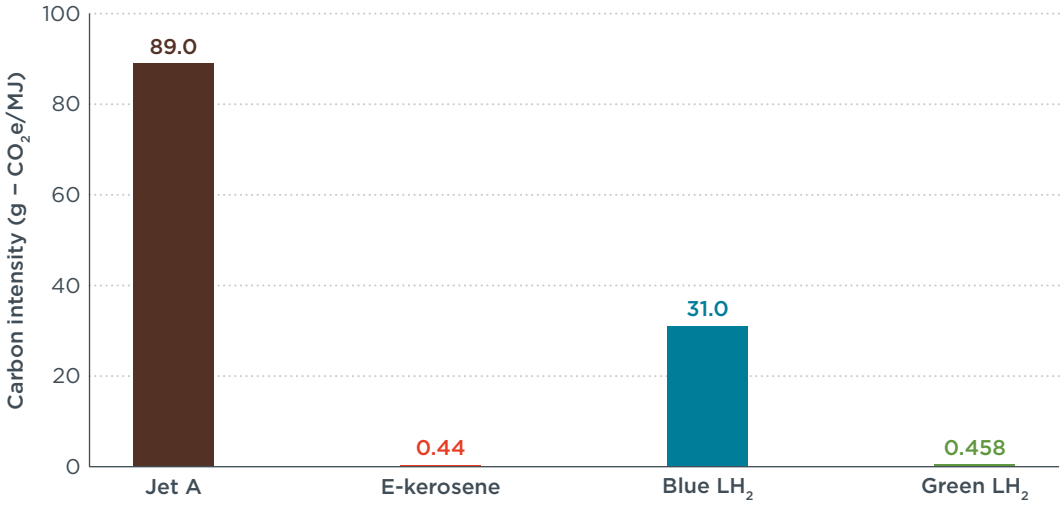

Figure 1. Carbon intensity of fuels investigated

The values for the carbon intensities of these fuels can be seen in Figure 1. The CORSIA baseline life-cycle emission value of 89 g-CO_2e/MJ is used for Jet A (International Civil Aviation Organization (ICAO), 2018). For blue LH_2, a carbon intensity of 31.0 g-CO_2/MJ is used (Zhou et al., 2021). This is the best-case scenario for the Natural Gas SMR + CCS pathway with additional energy requirements for liquefaction.[12] The carbon intensity for blue LH_2 can vary based on the assumptions made for the production process. A range from 31 g-CO_2e/MJ (with 99.9% carbon capture rate) to 127 g-CO_2e/MJ (with 20% upstream methane leakage rate) is possible.[13]

E-kerosene's life-cycle emissions are estimated at 0.44 g-CO_2e/MJ using the Greenhouse Gases, Regulated Emissions, and Energy Use in Transportation (GREET) model (Argonne National Laboratory, 2020). This assumes 100% additional renewable energy is being used, and the carbon is being captured from a point source. If DAC is required, the life-cycle emissions for e-kerosene increases to 4.1 g-CO_2e/MJ (Argonne National Laboratory, 2020). For this work we use the optimistic scenario of 0.44 g-CO_2e/MJ. For green LH_2, it is assumed that the production and liquefaction are powered by 100% additional renewable energy. This equates to 0.46 g-CO_2e/MJ of hydrogen burned.

While the potential life-cycle emissions of e-kerosene and green hydrogen are comparable, the total energy efficiency of the process will be different, owing to the extra energy needed to capture carbon and synthesize a hydrocarbon fuel. Based on the fuel conversion efficiency for hydrogen and e-kerosene from Brynolf et al. (2018) and the energy requirement for hydrogen liquefaction and carbon capture from GREET, we calculate the net energy ratio—the ratio of the usable fuel energy to the energy input into the production process—to be 56% for LH_2, 51% for e-kerosene using point source CO_2, and 46% for e-kerosene using DAC. Put another way, e-kerosene produced using DAC would require about 20% more energy to produce than LH_2 after considering all production energy, including hydrogen liquefaction.

For the fuel price analysis, we look at the expected costs in 2035 and 2050 in the United States and the European Union (EU), two likely early markets for hydrogen aircraft. The LH_2-powered aircraft would enter service in 2035, while 2050 is the target year for net-zero goals in aviation (Air Transport Action Group (ATAG), 2021; Federal Aviation Administration (FAA), 2021). The price for Jet A is taken from the United States Energy Information Administration reference-case projections (U.S. Energy

12 From the reference, a carbon capture rate of 99.9% (the CO_2 generated during hydrogen production) and an upstream methane leakage rate of 0.52% (from natural gas extraction and transportation).

13 These values are derived from the analysis in Zhou et al. (2021) but with the additional energy requirement for hydrogen liquefaction.

Information Administration, 2021). Costs for e-kerosene, blue LH_2, and green LH_2 are from Zhou & Searle (forthcoming) and Zhou et al. (forthcoming). The fuel prices are shown in Figure 2 in units of US dollars per megajoule (MJ) of energy.[14]

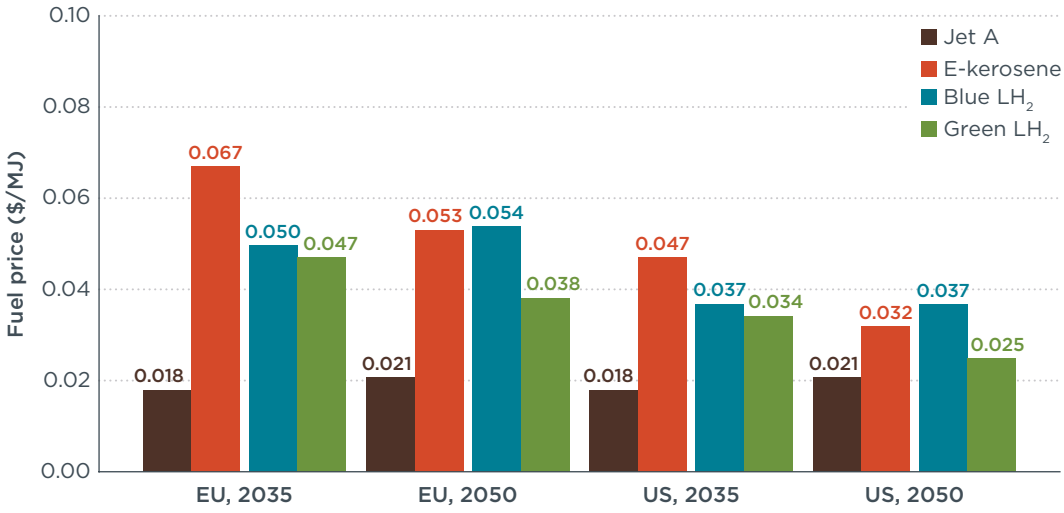

Figure 2. Fuel price by region, 2035 and 2050.

In aviation, the normalizing metric of choice is RPK. The energy intensity of the aircraft, expressed as the energy required per RPK (MJ/RPK), varies with mission length and aircraft type. The hydrogen-powered aircraft are found to have higher energy intensity than their hydrocarbon-powered equivalents. To compare them accurately, the length of the mission is kept constant, and the energy efficiency of the different aircraft types are used to express the carbon intensity and fuel price on a per-RPK basis. Details of the mission profile and the choice of reference missions are presented in Appendix B: Aircraft mission profile.

14 The fuel prices for Jet A and e-kerosene represent wholesale prices whereas the prices for blue and green LH_2 include transportation cost to the airport and represent the at-the-pump cost. The transport cost for Jet A and e-kerosene would be small due to the existing pipeline transport system to airports. Crucially, the hydrogen prices do not include the cost of building the refueling infrastructure at airports. Estimating these costs is difficult, so for the purpose of this work, we assume that those costs are subsidized by governments at early-adopter airports. If this is not the case, and customers are instead required to bear the cost of investments in hydrogen fueling infrastructure at airports, the price of blue and green LH_2 could increase substantially.

RESULTS

The main results of this work follow. First, we present the two LH_2-powered aircraft designs that were generated using the methods outlined above. Their performance, in terms of payload, range, and energy intensity, is compared to the performance of the reference aircraft on a variety of missions. Next, we quantify the emissions impact and the fuel costs of using blue and green hydrogen for the LH_2-powered designs, against using Jet A and e-kerosene for the reference aircraft. We end by estimating the size of the addressable market for the LH_2- powered designs based on 2019 operations, projecting the market's growth to 2035 and 2050 and quantifying the required hydrogen production and CO_2 mitigation potential based on varying aircraft adoption rates.

AIRCRAFT DESIGN

The primary constraint in the aircraft design is feasibility. Special focus is kept on designing aircraft that can fit within existing airline operations.

Turboprop

With no recent clean-sheet redesigns for turboprops, an improved wing design supported by low-fidelity analysis yields a more efficient aircraft. Using SUAVE, variable sweeps in the main wing's span, aspect ratio (AR), and taper ratio were performed.[15] We use the energy required per revenue passenger kilometer (MJ/RPK) as the efficiency metric. A lower value of MJ/RPK indicates a more fuel-efficient aircraft.

To ensure operational feasibility without higher-fidelity analyses, the ATR 72's wing loading of 415 kg/m^2 is used as a constraint. The final design parameters are shown in Table 3. The LH_2 turboprop fuselage is kept shorter than that of the Dash8 (< 32.8 m) as the aircraft's MTOM already increases by 24% at this fuselage length. Both the ATR 72 and the Dash8 fall under the 4C ICAO Aerodrome classification, which limits the wingspan to less than 36 m and the TOFL to less than 1,800 m.

Table 3. LH_2 aircraft design parameters

	ATR 72	LH_2 Turboprop	A320neo	LH_2 Narrow-body
Fuselage length (m)	27.17	32.02	37.57	44.51
Wingspan (m)	27.05	32.5	35.8	35.8
AR	12	15	10	10
Mean aerodynamic chord (m)	2.34	2.43	3.63	4.01
Taper ratio	0.5	0.25	0.27	0.25
Passengers	70		165	
Cruising Mach number	0.452		0.78	
Cruising altitude (ft)	20,000		35,000	

Figure 3 presents a visualization of the LH_2-powered turboprop aircraft with cut-outs showing the layout of the fuselage. The tank, fuselage, wing, and tail are drawn to scale. The hydrogen tank is placed behind the passenger cabin. This moves the center-of-gravity of the aircraft aft. Consequently, maintaining the tail-volume coefficient of the reference aircraft requires a larger tail empennage. The wing is also moved aft along the fuselage to keep the aircraft's neutral point behind its center of gravity and ensure static stability (MIT OCW, 2006).

15 These variables trade off improving the aircraft's lift-to-drag ratio against increased MTOM due to added structural mass. Increasing the lift-to-drag ratio improves the aircraft's fuel efficiency and range, while increasing the MTOM reduces the fuel efficiency and range. The optimal design balances out these countervailing effects.

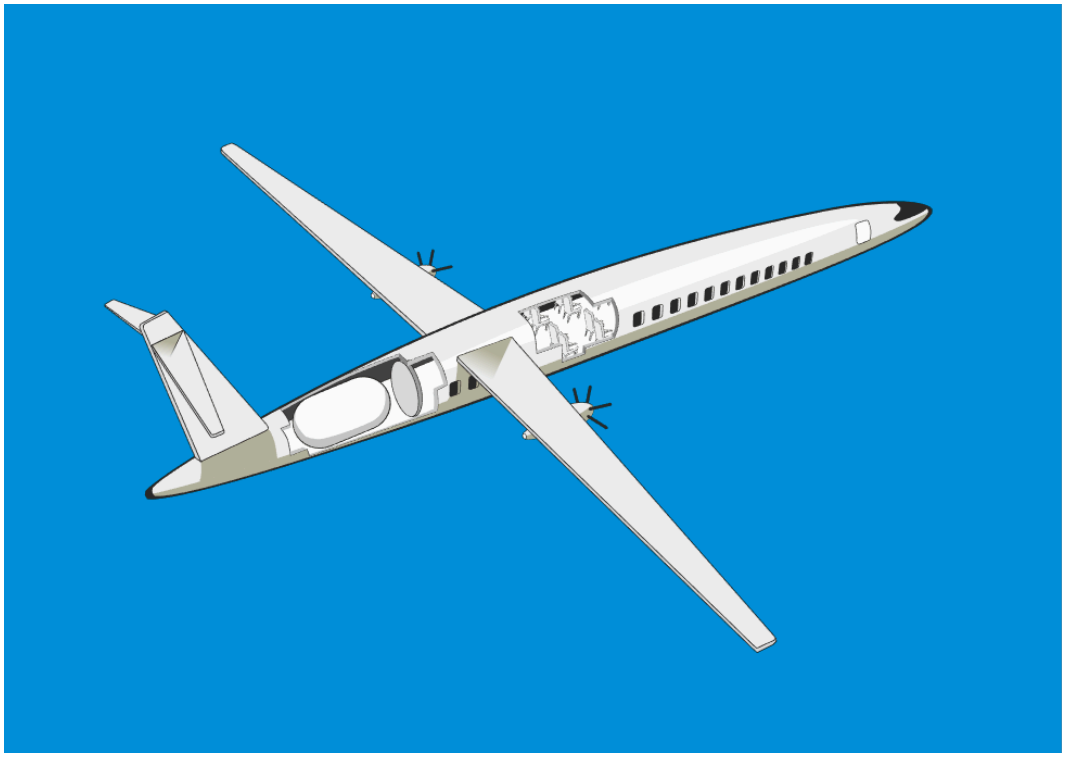

Figure 3. Representation of the tank and passenger cabin layout for the LH_2-powered turboprop

Narrow-body turbofan

Narrow-body turbofan aircraft are updated periodically due to their popularity and widespread use. Recent generations have not been clean-sheet designs but instead derivative aircraft with newer engines, more composite utilization, and improvements to the wing design, particularly at the wingtips. The reference aircraft, the A320neo, falls under the 4C ICAO Aerodrome classification which does not place a limit on the TOFL (>1,800 m) but restricts the wingspan to 36 m. The A320neo is already at this limit with a wingspan of 35.8 m. This, in addition to the more recent improvements to the aircraft, means that no efficiency improvements can be gained by low-fidelity aircraft analysis. Consequently, the final design parameters are nearly identical to the reference aircraft as presented in Table 3.

Figure 4 presents the LH_2-powered narrow-body. As with the turboprop visualization, the fuselage, wing, tank, and tail are drawn to scale. The hydrogen tank is placed behind the passenger cabin. Similar stability- and control-related concerns necessitate a larger tail empennage and a further aft mounting of the wing.

Figure 4. Representation of the tank and passenger cabin layout for the LH_2-powered narrow-body

REFERENCE MISSION SIMULATIONS

Maximum range missions

To determine the maximum range of the aircraft, we iterate on the cruise distance until the landing fuel mass is exactly what would be required for fuel reserves. Simulations are carried out using the design payload of 70 and 165 passengers for the turboprop and narrow-body, respectively. For the fossil-fueled aircraft, the takeoff fuel load is determined by subtracting the sum of the OEW and the payload weight from the MTOM. For the LH_2-powered aircraft, the maximum possible fuel load is carried. Simulations are run using GI of 0.2 and 0.35 for the LH_2 fuel system and the results for the two LH_2-powered aircraft are compared to the reference aircraft. The seat pitch is kept at 30 inches (0.764 m) for the reference mission simulations.

For the turboprop (Table 4), the LH_2-equivalent incurs significant weight penalties of 24% and 10% increases in MTOM for a fuel system GI of 0.2 and 0.35, respectively. The difference in the fuel mass and the fuel system mass between the LH_2- and Jet A-fueled aircraft shows how the lower mass of LH_2 is overshadowed by the mass of the fuel system. The resulting increase in MTOM limits the size of the fuel tank, which in turn reduces the range of the aircraft. It also increases the energy intensity of the design by 10% to 20%, with the higher GI corresponding to a more fuel-efficient aircraft. However, these aircraft can still comfortably cover >90% of the missions flown by the ATR 72.

Table 4. Weights, range, and fuel intensity of the turboprop aircraft

	ATR 72	LH_2 Turboprop	
		GI = 0.2	GI = 0.35
OEW (kg)	13,500	20,900 (+55%)	17,800 (+32%)
Fuel system mass (kg)	222[16]	4,750 (+2,037%)	2,200 (+892%)
Fuel mass (kg)	3,150	1,190 (-62%)	
MTOM (kg)	23,000	28,600 (+24%)	25,500 (+10%)
Range (km)	1,530	1,220 (-19%)	1,420 (-7%)
Fuel intensity (MJ/RPK)	0.854	1.03 (+20%)	0.936 (+10%)

The results for the narrow-body turbofan are presented in Table 5. The LH_2-powered aircraft falls well short of the range capabilities of the A320neo. Here, rather than MTOM being the constraint, the maximum allowable fuselage length limits the size of the LH_2 tank and, therefore, the range. This range concern is mitigated by the fact that narrow-body aircraft are largely used for routes that are less than 3,180 km. The limited tank size leads to a moderate increase in MTOM of 15% for a GI of 0.2, and a 3% decrease in MTOM for the GI of 0.35.

Table 5. Weights, range, and fuel intensity of the narrow-body aircraft

	A320neo	LH_2 Narrow-body	
		GI = 0.2	GI = 0.35
OEW (kg)	44,300	70,100 (+56%)	56,000 (+26%)
Fuel System Mass (kg)	286	20,200 (+6,968%)	9,390 (3,181%)
Fuel Mass (kg)	19,100	5,050 (-73%)	
MTOM (kg)	79,000	90,800 (+15%)	76,702 (-3%)
Range (km)	5,140	2,800 (-46%)	3,440 (-33%)
Fuel intensity (MJ/RPK)	0.864	1.09 (+26%)	0.911 (+5%)

Representative missions

Aircraft are often flown on routes that are well below their maximum range capability. Ninety percent of the ATR 72's 2019 routes are less than 750 km in length,[17] while the aircraft has a claimed range of double that distance, at 1,528 km (ATR, 2020). Similarly, the A320neo has a claimed range of 6,500 km but 90% of its missions in 2019 were shorter than 3,180 km. Consequently, to compare the energy and carbon intensities of the LH_2 and the reference aircraft, we fly them on missions that represent the median (half of missions above, and half below) and 90th-percentile mission distance. Table 6 and Table 7 present the results for the turboprop and the narrow-body turbofan, respectively. The carbon emissions and price values are for untaxed Jet A and green LH_2 produced in the US in 2050.

As with the maximum range simulations, the LH_2-powered aircraft exhibit higher MJ/RPK energy intensities. The energy efficiency penalty of hydrogen is exacerbated on shorter flights because the effective GI of the LH_2 fuel system decreases when the fuel system is not filled to maximum capacity; the LH_2 design carries the excess fuel tank weight on all its flights while the Jet A aircraft can fly lighter on shorter

16 The fuel system mass estimate for the Jet A-powered aircraft (ATR 72 and A320neo) comes from Piano 5.

17 This is determined by looking at all the routes flown by the ATR 72 in 2019 using the GACA database (Graver et al., 2020) and calculating the 90th-percentile of the route distances. An identical analysis is performed for the Airbus A320neo. The median route distance is used as well.

missions by loading less fuel. For the most conservative GI of 0.2, the LH_2-powered narrow-body has a maximum range of 2,800 km, which is too short for the 90% coverage mission. However, the aircraft still covers the distance of 82% of the routes the A320neo flew in 2019.

Table 6. Energy and emissions intensity of the turboprop aircraft

Mission	Parameter	ATR 72	LH_2 Turboprop with green hydrogen	
			GI = 0.2	GI = 0.35
Median mission 400 km 70 PAX	Fuel burn (kg)	619	269 (-57%)	240 (-61%)
	MJ/RPK	0.96	1.15 (+20%)	1.03 (+8%)
	g-CO_2e/RPK	85.1	0.528 (-99%)	0.472 (-99%)
	$ fuel/RPK (US, 2050)	0.020	0.029 (+45%)	0.026 (+30%)
90% mission 750 km 70 PAX	Fuel burn (kg)	1,080	466 (-57%)	423 (-61%)
	MJ/RPK	0.89	1.06 (+20%)	0.97 (+9%)
	g-CO_2e/RPK	78.9	0.488 (-99%)	0.444 (-99%)
	$ fuel/RPK (US, 2050)	0.018	0.027 (+45%)	0.024 (+32%)

Table 7. Energy and emissions intensity of the narrow-body turbofan aircraft

Type	Parameter	A320neo	LH_2 narrow-body with green hydrogen	
			GI = 0.2	GI = 0.35
Median mission 1,500 km 165 PAX	Fuel burn (kg)	4,461	2,230 (-50%)	1,850 (-59%)
	MJ/RPK	0.78	1.06 (+36%)	0.88 (+13%)
	g-CO_2e/RPK	69.3	0.487 (-99%)	0.403 (-99%)
	$ fuel/RPK (US, 2050)	0.016	0.027 (+64%)	0.022 (+36%)
90% mission 3,180 km 165 PAX	Fuel burn (kg)	9,920	-	3,970 (-60%)
	MJ/RPK	0.82	-	0.91 (+11%)
	g-CO_2e/RPK	72.8	-	0.412 (-99%)
	$ fuel/RPK (US, 2050)	0.017	-	0.023 (+34%)

The 90% mission for the narrow-body turbofan aircraft is used to perform more detailed analysis of different fuels. This mission is chosen as it would cover the largest number of RPKs and similar trends are seen for all other missions explored here. The A320neo is used for the hydrocarbon fuels, Jet A and e-kerosene. The LH_2-powered narrow-body with a GI of 0.275 (the middle of the 0.2-0.35 range of GI) is used for green and blue LH_2.

Figure 5 shows the carbon intensity, in grams of CO_2 equivalent emitted per RPK (g-CO_2e/RPK), for the two aircraft types and fuels. Even with the higher energy intensity in MJ/RPK of the LH_2 aircraft, the best case blue LH_2 (99.9% carbon capture rate) emits about 40% the g-CO_2e per RPK of Jet A. Using less optimistic assumptions for the blue hydrogen pathway would further degrade its benefits; for example, under the mean (63.71 g-CO_2e/MJ), blue hydrogen would only reduce emissions by 14% compared to Jet A. Green LH_2 and e-kerosene, on the other hand, have near-zero carbon intensities per RPK.

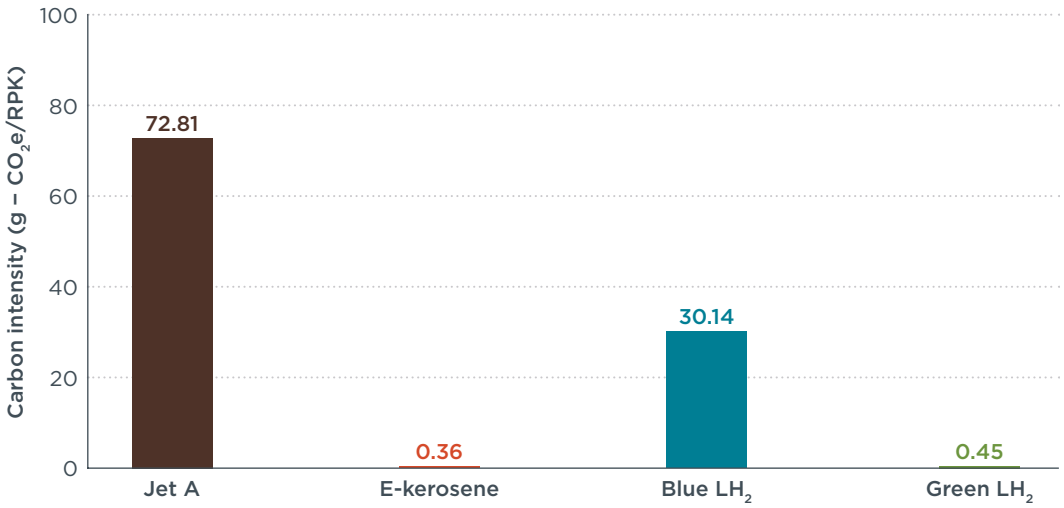

Figure 5. Narrow-body aircraft carbon intensity by fuel type, GI = 0.275.

These aircraft carbon intensities, combined with the fuel price assumptions above, were used to explore the fuel costs of the reference and LH_2-powered aircraft by region and year. The price of fuel varies geographically and temporally. Figure 6 presents the fuel costs per RPK for the United States and the European Union in 2035 and 2050. The solid bars represent the baseline price while the diagonally hatched bars represent the effect of $200 and $400 price per tonne of CO_2 emitted.

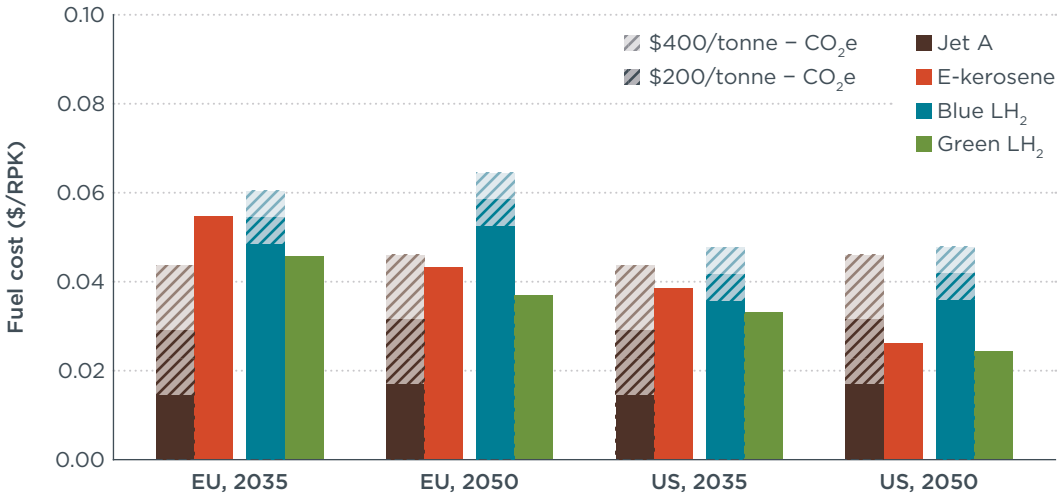

Figure 6. Fuel cost by region, 2035 and 2050, with and without carbon pricing.

Several conclusions can be drawn from the figure. First, in the long-run (2050), blue LH_2 is expected to be the most expensive fuel, followed by e-kerosene, then by green LH_2 and Jet A. Second, in all cases, carbon pricing will be needed to close the price gap between green LH_2 and fossil jet fuel. In the United States, green LH_2 becomes cheaper than Jet A in 2035 with a $256/tonne-$CO_2$e tax, but only requires a $102/tonne-$CO_2$e tax in 2050 to be cost-competitive. In the European Union, higher expected hydrogen production costs mean that a larger carbon price ($277/tonne-$CO_2$e tax) will be needed in 2050 for green LH_2-powered aircraft to be cost-competitive. As a point of reference, the implied carbon price for transport fuels under California's Low Carbon Fuel Standard today is about $200/tonne (California Air Resources Board, 2021).

Arguably, the real comparison for green LH_2 is with e-kerosene. The aviation industry is adopting Net Zero by 2050 targets (Air Transport Action Group (ATAG), 2021; Federal Aviation Administration (FAA), 2021) which would require large amounts of SAF

uptake. This is also reflected in the proposed ReFuel EU regulations that would require 20% SAF (5% synthetic aviation fuels) in 2035 and 63% SAF (28% synthetic aviation fuels) in 2050 (European Commission, 2021a). Under the current cost assumptions, green LH_2 is expected to be a cheaper fuel than e-kerosene for the missions investigated. This price-advantage could be smaller or reversed when accounting for the cost of building hydrogen refueling infrastructure at airports. On the other hand, the cost of e-kerosene production could increase if the more energy-intensive DAC (rather than point source carbon capture) is required.

ADDRESSABLE MARKET

This section tackles the question of what share of existing missions could be replaced by LH_2-powered aircraft. We also investigate potential changes to the aircraft's carrying capacity to improve its mission coverage capability. This requires the use of payload-range diagrams which illustrate the trade-off between the number of passengers aboard an aircraft and the range it can fly with that payload. If the aircraft is not completely full, it can fly a longer distance than if it is completely full. To compare missions we use the total number of seats available on the route, regardless of whether they are filled or not. This builds in a buffer for the expected passenger fill percentage for the airline and does not assume a fully loaded aircraft for every mission. While there would be the option to carry freight if the LH_2-powered aircraft are not completely full, freight carried in the belly of passenger aircraft is not modeled.

For each aircraft type, different passenger capacities are explored to identify the maximum mission coverage. The seat pitch is varied between 0.737 and 0.762 m (29 and 30 inches) and the GI values are varied between 0.2 and 0.35. Additionally, we simulate LH_2-powered aircraft families where the passenger capacity and tank size are traded to either increase range at a lower passenger capacity or increase passenger capacity at the expense of maximum range.

Turboprop

To determine the addressable market, all turboprop missions are compared to the payload-range capability of the aircraft.[18] Figure 7 plots each route flown by a turboprop as a dot, where the x-location represents the distance of the route, and the y-location represents the number of seats available on the aircraft that flew the route. The dots are colored green if they lie within the payload-range capability of the LH_2-powered turboprops, or red if the mission is beyond the aircraft's capability. There is distinct banding of the dots horizontally as a specific type of aircraft will have a fixed number of seats but will fly routes of varying lengths.

The yellow line represents the payload-range diagram of the ATR 72. The blue, brown, and red lines represent the payload-range diagrams of LH_2-powered turboprops of the given passenger capacities.[19] In creating these different configurations, a maximum LH_2 tank length of 3.5 m is imposed to limit the increase in the aircraft's MTOM. The fuselage length limit is also imposed but is only active for the largest payload aircraft. The 70-seat variant is the original design investigated earlier, but the 78- and 50-seat aircraft are analyzed to see if they can cover a larger percentage of RPKs. In this case,

18 Only turboprop missions are considered, as opposed to all regional missions, because a turboprop aircraft would not replace a turbofan-powered regional aircraft which can fly at a higher cruise speed. A turbofan can fly at Mach 0.78 and can cover a mission ~1.5x faster compared to a turboprop that flies at Mach 0.45.

19 The payload-range diagram of the ATR 72 has an additional corner which is absent from those of the LH_2-powered aircraft. This is because fossil-fueled aircraft at their MTOM and maximum payload capacity (first corner) are often not at their maximum fuel capacity. Consequently, when the payload is reduced, more fuel can be added to keep the aircraft at its MTOM, and the aircraft's range keeps increasing. This continues until the aircraft reaches its maximum fuel capacity (second corner). Beyond this, no additional fuel can be added and the payload-range diagram falls rapidly as the payload is reduced without adding fuel to increase range. In contrast, the LH_2-powered aircraft at their MTOM are at maximum payload and fuel capacity (first and only corner). When the payload capacity is reduced, fuel cannot be added to keep the aircraft at MTOM. Consequently, the payload-range diagram starts falling rapidly.

the 78-seat variant has the maximum coverage and, by itself, can replace 86% to 96% of the 64 billion RPKs flown by turboprops in 2019.[20] If this LH_2-powered aircraft were to replace all these missions and run on green LH_2, it would mitigate 9.6–10.4 million tonnes of CO_2e ($Mt\text{-}CO_2e$) emissions in 2019. This would be 1.0–1.1% of the 955 $Mt\text{-}CO_2e$ attributable to passenger aviation in 2019 (Graver et al., 2020).[21]

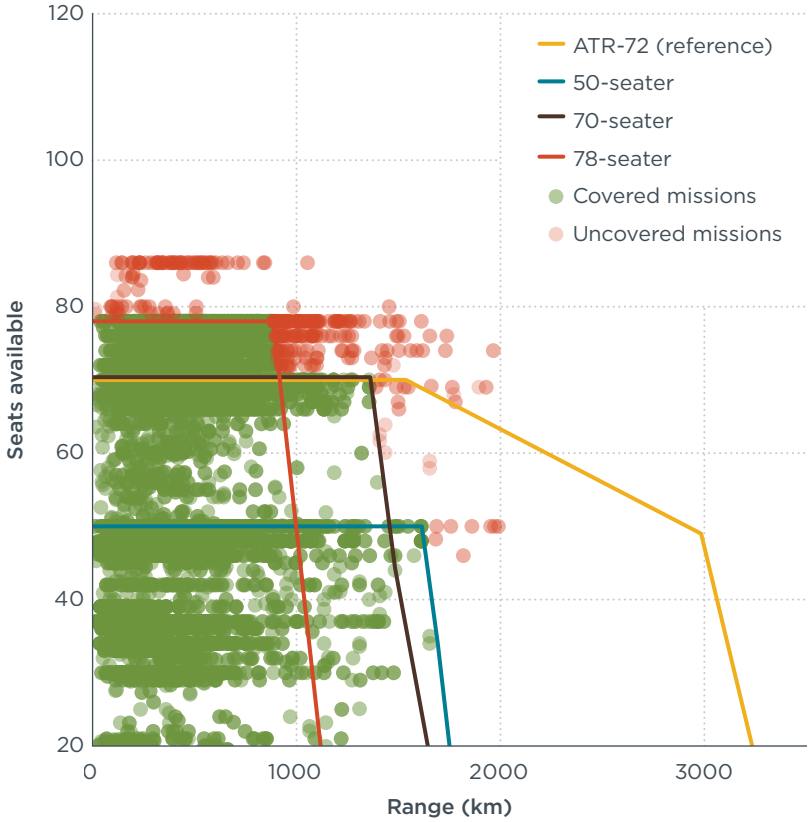

Figure 7. 2019 turboprop missions compared to the payload-range capability of LH_2-powered turboprop (GI = 0.275, SP = 30 in.)

These numbers increase slightly when using a family of aircraft. The RPK coverage for the different combinations of GI and seat pitch (SP) for the single aircraft and the family of aircraft are compared in Figure 8. The significant trends are that increasing the GI (resulting in a lower fuel system mass) and reducing the seat pitch (resulting in more space for the fuel tank) improve the RPK coverage. Both those factors increase the aircraft's range at a constant payload, which results in the increased coverage. While the aircraft family does not significantly change the coverage, there is still merit in creating an aircraft family. Using a 78-seat aircraft to service missions that usually carry < 50 passengers would be inefficient and economically unfavorable for airlines.

20 Range of values depend on the fuel system's GI and the seat pitch.

21 The 785 $Mt\text{-}CO_2$ value in the reference uses a carbon intensity of 73.15 gCO_2/MJ for Jet A. This is scaled to 955 $Mt\text{-}CO_2e$ by taking into account upstream emissions for fuel production using CORSIA's carbon intensity value of 89 gCO_2e/MJ for Jet A.

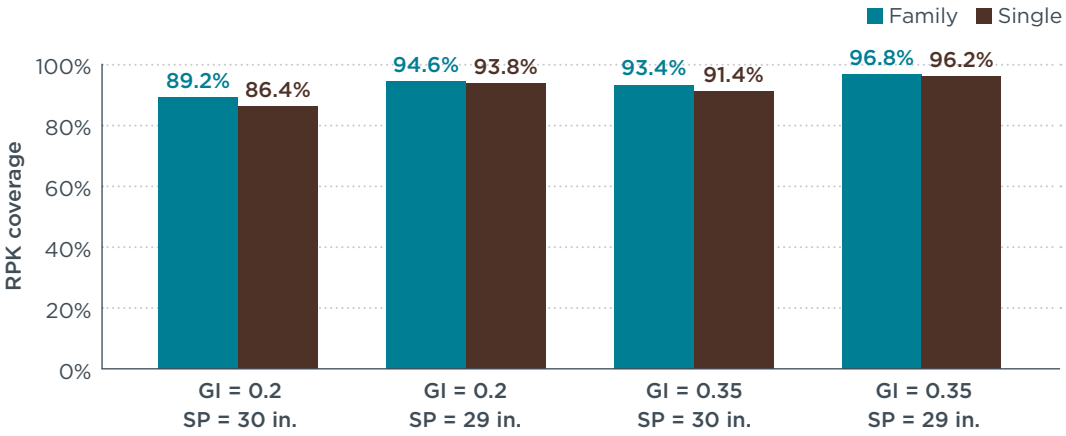

Figure 8. Percentage of turboprop RPKs covered by LH_2-powered aircraft

Narrow-body turbofan

A similar analysis is carried out for the LH_2-powered narrow-body turbofan. Figure 9 plots the 2019 narrow-body routes as dots. The dots are colored green if they are replaceable by the LH_2-powered aircraft, or red if the mission is beyond the aircraft's capability. Due to the large number of narrow-body missions, the routes are grouped together such that each individual dot represents 4.6 billion RPKs. Five different seat configurations are examined, ranging from 140 to 200 seats. The performance of the A320neo is shown as the purple line.[22]

All combinations of the 5 configurations are checked to see which three aircraft combination provides the best RPK coverage. A combination of the 150-, 168- and 192-seater would provide the largest RPK coverage for an aircraft family, while the largest and smallest variants would only marginally increase coverage. Individually, the 192-seater provides the largest RPK coverage. The relative coverage values are shown in Figure 10, clustered by GI and seat pitch, and colored by single aircraft vs. a family of aircraft. As with the turboprop, increasing the GI and reducing the seat pitch increase the aircraft's range and result in greater RPK coverage. For this class of aircraft, the family approach provides a significant improvement in coverage. If these LH_2-aircraft were to take over all the replaceable routes and were run on green LH_2, they could mitigate 229 to 338 Mt-CO_2e in 2019. This represents about 23% to 35% of the 955 Mt-CO_2 attributable to passenger aviation in 2019.

22 As with the turboprops, the A320neo payload-range diagram has a second corner representing its range at MTOM with maximum fuel load, but the LH_2-powered aircraft at MTOM are already at maximum fuel load. The maximum passenger capacity of 180 for the A320neo is higher than the design payload of 165 passengers used in the reference missions.

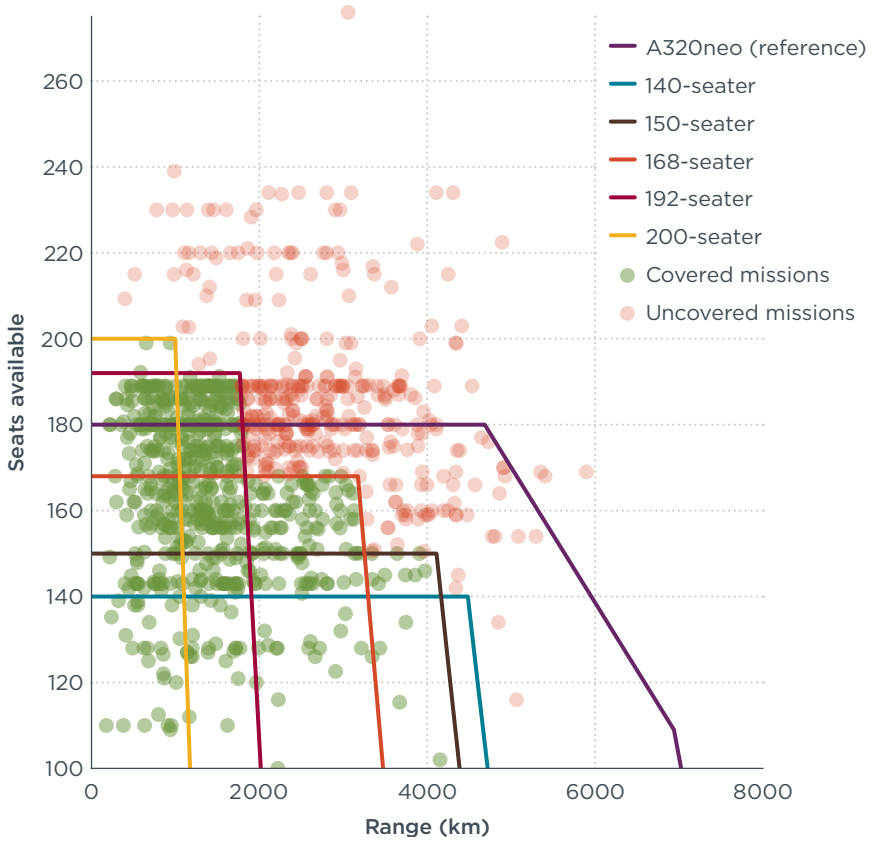

Figure 9. 2019 narrow-body missions compared to the payload-range capability of an LH_2-powered narrow-body (GI = 0.275, SP = 30 in.)

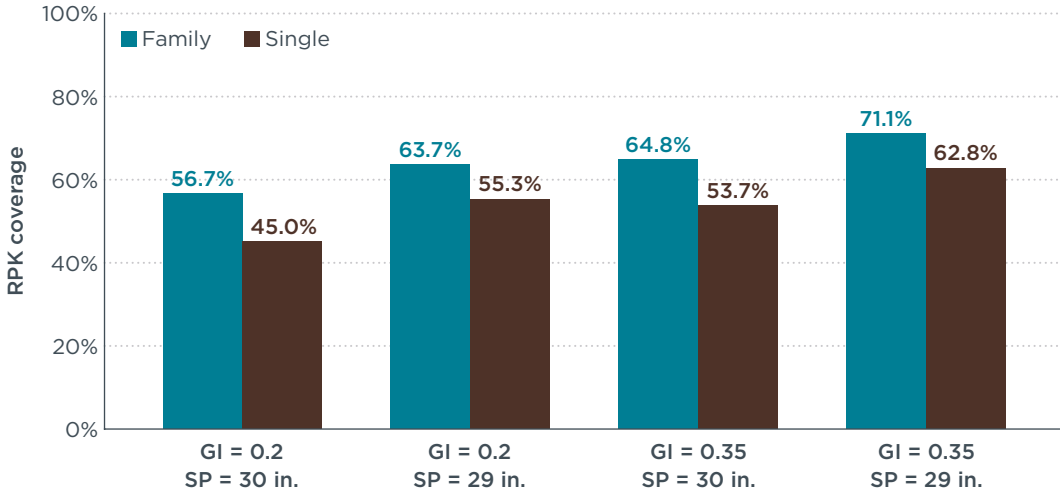

Figure 10. Percentage of narrow-body RPKs covered by LH_2-powered aircraft

Combining the RPK coverage of the turboprop and the narrow-body aircraft families, the addressable market as a percentage of the total passenger aviation market is presented in Figure 11. The narrow-body family can cover a much larger share of commercial operations than the turboprop family. While the LH_2-powered turboprop can replace nearly all current turboprop operations, most passenger RPKs are flown on larger narrow-body aircraft. As a result, while capable of replacing only two-thirds of current narrow-body operations, the LH_2-powered narrow-body family can cover about one-third of the total passenger aviation market. This highlights the value of prioritizing narrow-body LH_2 aircraft development.

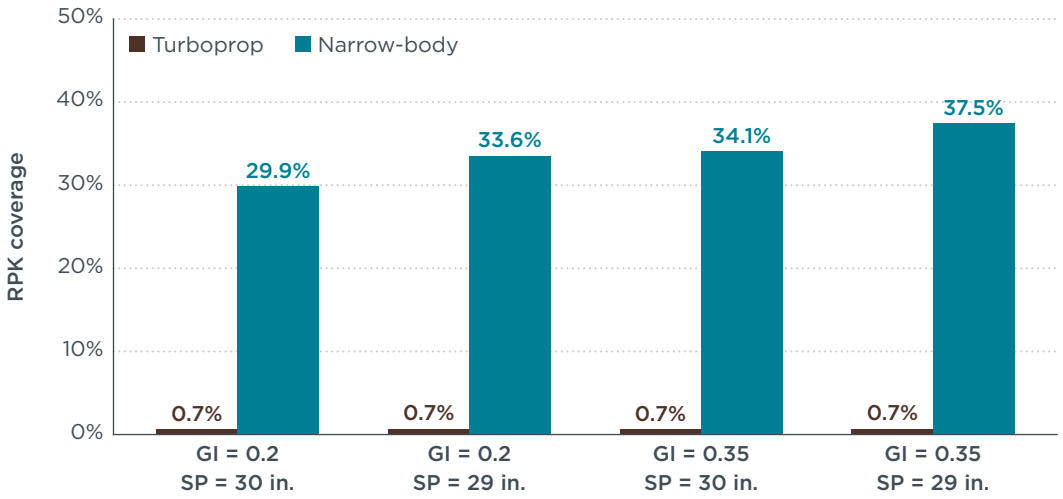

Figure 11. Total RPK coverage of LH_2 aircraft families by aircraft class, GI, and seat pitch

There is still value in developing a hydrogen-powered turboprop, which has the potential to enter the aviation market sooner than the narrow-body, with demonstration flights slated for as early as 2026 (ZeroAvia | Alaska Air Group | Hydrogen Powertrain, 2021). That design will be fueled by gaseous hydrogen powering a fuel cell. This approach could provide a crucial stepping stone for the aviation industry in the adoption of hydrogen as a fuel.

HYDROGEN PRODUCTION REQUIREMENTS

It is important to note that these RPK coverage and CO_2 mitigation numbers are based on 2019 air traffic but the earliest LH_2-powered aircraft are expected to enter service in 2035. Projecting historical trends from the GACA database, passenger air traffic is expected to grow worldwide at a compounded annual growth rate (CAGR) of 3.0% in the 2019–2050 timeframe. This is more conservative than the post-COVID traffic projection from ICAO which expects a CAGR of 3.6% (International Civil Aviation Organization (ICAO), n.d.).

With internal fleet turnover modeling that assumes new aircraft deliveries are proportional to the traffic growth rate, and that LH_2-powered aircraft make up 25% to 50% of new regional and narrow-body aircraft deliveries starting in 2035, we predict that 20% to 40% of addressable RPKs could be serviced by LH_2-powered aircraft in 2050. Figure 12 presents the potential demand for hydrogen by projecting the 2019 RPKs using the 3.0% CAGR and using different 2050 adoption rates, with aircraft adoption linearly interpolated starting in 2035. The 100% adoption line represents the radical case where all replaceable routes are serviced by LH_2-powered aircraft by 2050.

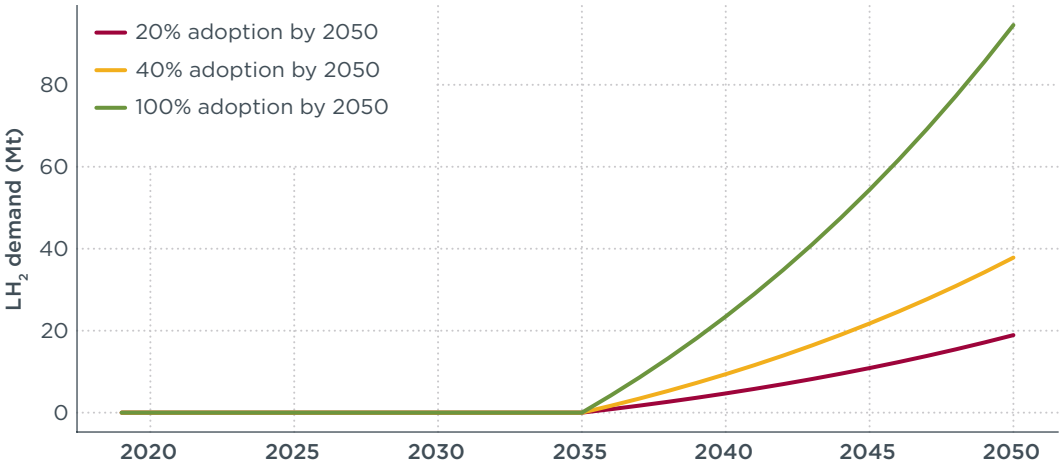

Figure 12. Demand projection for green LH_2 assuming different aircraft adoption rates

Green LH_2 demand under the lower adoption cases would be modest, on the order of 18.9 to 37.8 Mt per year. For the 100% adoption case, the demand for green LH_2 would grow to 62.3–94.6 Mt in 2050, depending on the precise combination of GI and seat pitch assumed. As a reference, the International Energy Agency estimates that 69 Mt of dedicated H_2 was produced worldwide in 2019 (International Energy Agency (IEA), 2019).[23] Of greater concern, less than 0.1% of that was produced using water electrolysis, which would be required for green LH_2 production.

The adoption rates are dependent on airports having hydrogen storage and delivery infrastructure. Initial operations will be limited to areas where the infrastructure is available. While the hydrogen production numbers for the 100% adoption rate case are expected to be over-estimates (because 100% adoption is unlikely by 2050), they are worth keeping in mind as markers of the effort required to support deep decarbonization of aviation through hydrogen-powered aircraft.

CO_2 MITIGATION POTENTIAL

An increase in RPKs flown on LH_2-powered aircraft operating on green hydrogen would translate to an increase in their CO_2 mitigation potential. While we forecast RPKs to grow at 3.0% annually, historical trends suggest that the fleet-averaged fuel burn for narrow-body and turboprop aircraft has decreased at 0.5% annually (Graver & Rutherford, 2018).

Using these values, we can project the mitigation potential of these LH_2-powered aircraft from 2035 and 2050. The maximum mitigation potential of 238–348 Mt-CO_2e/year based on 2019 operations grows to 353–516 Mt-CO_2e/year in 2035 and 510–745 Mt-CO_2e/year in 2050. The ranges of values are based on the GI of the fuel tanks, seat pitch, and whether a single aircraft or a family of aircraft is developed. No improvements to the hydrogen-powered aircraft after 2035 are assumed as these would be the first generation of their kind and substantial updates before 2050 seem unlikely.

Using the calculated adoption rates for these aircraft once deliveries start in 2035, we get CO_2 mitigation wedges that can be extrapolated to 2050. Figure 13 presents the impact of these aircraft between 2035 and 2050 under varying adoption rates. To reiterate, the 20% and 40% adoption rates are realistic, but the 100% adoption line represents a radical case where all replaceable routes are serviced by LH_2-powered aircraft running on 100% green hydrogen in 2050. It is instructive for understanding the maximum impact that evolutionary hydrogen-powered aircraft could have. With the

23 Dedicated production refers to the intentional manufacturing of hydrogen and does not include H_2 produced as a by-product.

20% to 40% adoption rate, LH_2-powered designs could mitigate 126 to 251 Mt of CO_2e in 2050 representing 6–12% of passenger aviation's CO_2e inventory. In the 100% adoption case, 628 Mt of CO_2e could be mitigated, representing 31% of passenger aviation's CO_2e inventory and capping passenger aviation emissions at 2035 levels. Thus, evolutionary LH_2 could cap, but not absolutely reduce, passenger aviation CO_2e emissions after 2035. Here, the mitigation potential is averaged over the different GI values, seat pitch values, and single vs. family of aircraft development.

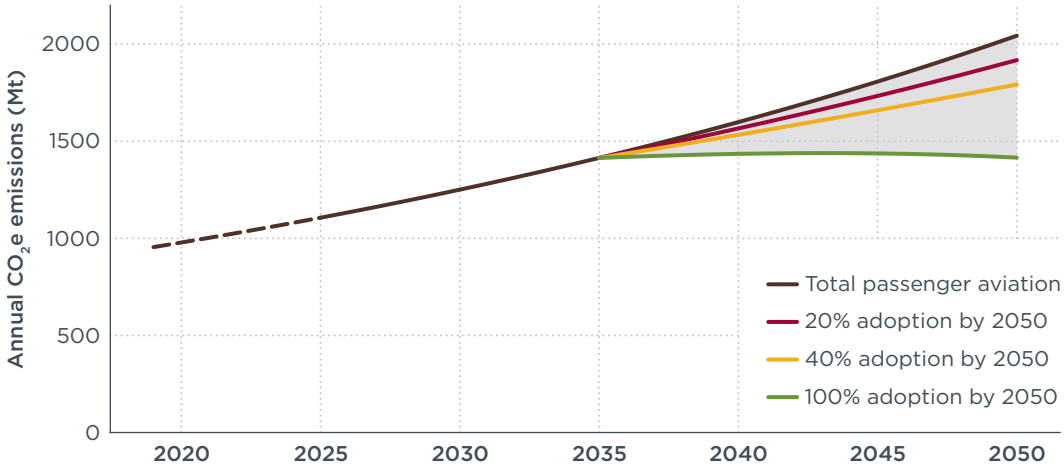

Figure 13. CO_2e emissions from passenger aviation under various scenarios of adoption of LH_2-powered aircraft, 2020 to 2050

CONCLUSIONS

We assessed the performance characteristics, operational potential, fuel costs, and CO_2e mitigation potential associated with evolutionary hydrogen-powered aircraft that could enter service by 2035. This led to the following high-level conclusions.

While LH_2-combustion aircraft do not perform as well as their jet fuel counterparts, they could still play an important role in aviation decarbonization. The evolutionary LH_2-combustion aircraft will be less capable—more energy intensive, with some payload and range limitations—relative to current Jet A counterparts. This is due to the low energy density of hydrogen and the high mass of fuel storage, as measured by achievable gravimetric indices (0.2 to 0.35). Still, even these aircraft can be impactful: the turboprop family could cover up to 97% of RPKs flown by turboprops over 2019, while a narrow-body turbofan aircraft family could cover up to 71% of narrow-body RPKs. This translates to 24% to 38% of total passenger aviation RPKs.

Under the most optimistic fuel and fleet turnover assumptions, evolutionary LH_2-powered aircraft could cap, but not absolutely reduce, passenger aviation CO_2 compared to 2035 levels. This would require all replaceable missions in 2050 to be serviced by LH_2-powered aircraft using green hydrogen and would result in mitigation of 628 Mt-CO_2e in 2050, representing 31% of passenger aviation's CO_2e emissions. Internal modeling suggests that a 20% to 40% adoption rate is realistically achievable and would mitigate 126 to 251 Mt-CO_2e in 2050, representing 6% to 12% of passenger aviation's CO_2e emissions. Other technologies, including more fuel-efficient aircraft and sustainable aviation fuels, along with measures to moderate traffic growth, will be needed to meet airlines' aggressive climate goals.

Fueling LH_2 designs with green hydrogen is expected to cost more than fossil jet fuel but less than using blue hydrogen or e-kerosene. While the market for LH_2 aircraft could be broad, powering it with green LH_2 will increase fuel costs compared to conventional Jet A aircraft. Carbon pricing would be needed to make green LH_2 cost-competitive, with breakeven compared to Jet A expected at between $102 and $277/tonne CO_2e in 2050, depending on geography. However, given the industry-wide push toward non-biomass SAFs, synthetic fuels like e-kerosene would likely be a better cost comparison for hydrogen than Jet A, especially from 2035 onwards. Our results suggest that green LH_2 will be cheaper than e-kerosene on routes up to 3,400 kilometers.

To the extent that manufacturers need to prioritize aircraft development, a focus on narrow-body LH_2-powered designs is recommended to provide the highest potential emissions coverage. Narrow-body aircraft are responsible for more than half of all aviation RPKs flown today. While LH_2-powered narrow-body aircraft cannot completely replace its fossil-fueled alternative, they could cover almost two-thirds of the narrow-body market, which translates to one-third of the total passenger aviation market. In contrast, an LH_2-powered turboprop can replace most of the existing turboprop market, however it would cover less than 1% of the total passenger aviation market.

Proper life cycle accounting, along with policies to attract green hydrogen with low life cycle emissions to aviation, will be needed to maximize the mitigation potential for LH_2 aircraft. The full decarbonization potential of LH_2-powered aircraft suggested in this work is only achievable if the aircraft are fueled by green LH_2 produced using 100% additional renewable energy. While green hydrogen can have near-zero life cycle emissions, even with optimistic assumptions for carbon capture (99.9%), blue hydrogen can provide at most a two-thirds reduction compared to Jet A. Under less optimistic assumptions, much of the benefit of blue hydrogen would be lost. Therefore, policies promoting the use of green LH_2 in these aircraft will be necessary to realize their fullest CO_2 mitigation potential.

Advances in key technology parameters can improve the economic case for LH_2-powered aircraft. Improvements in LH_2 storage technology to increase GI would reduce the weight of the fuel system, thereby boosting range, reducing fuel use and cost, and growing the addressable market. Research and development into hydrogen-combustion turbines could reduce fuel burn and improve the aircraft's range. Improvements in the hydrogen production process, such as an increased electrolyzer efficiency, would reduce its net energy ratio and drive down its price.

Supportive government policies will be needed if LH_2-powered aircraft are to succeed. These include carbon pricing, low-carbon fuel standards, or alternative fuel mandates to bridge the cost gap with fossil jet fuel, and life cycle accounting to ensure that aviation has access to the cleanest sources of hydrogen. Public support for research and development of key hydrogen technologies such as LH_2 storage tanks and hydrogen-combustion turbines is also recommended. Investment in hydrogen production, distribution to airports, and aircraft refueling technology will bolster the economic case for hydrogen-powered aircraft, while policies to accelerate fuel efficiency, for example a coordinated phase out of aircraft that fail ICAO's aircraft CO_2 standard, could create new market pull for hydrogen aircraft following their entry into service.

This research has highlighted several potential areas for further study. This work does not consider the capital investment needed to develop hydrogen aircraft or to build hydrogen fueling infrastructure for the hydrogen-powered aircraft at the airport. An important next step would be to determine where and how to invest in hydrogen infrastructure to maximize the CO_2 mitigation potential while minimizing cost. However, even if the infrastructure is in place and the aircraft are built, more detailed modeling of fleet turnover to determine the likely pace of market penetration of the LH_2-powered aircraft would be required to quantify the real-world CO_2 mitigation of these new aircraft.

Aircraft stability is not considered in this study but modeling the forward shift of the center-of-gravity as LH_2 gets burned is an essential step in ensuring feasibility of the design. The capabilities of a fuel cell powered aircraft using GH_2 should also be assessed, particularly in the regional turboprop segment. The higher efficiency of a fuel cell and electric drivetrain could make it a promising alternative to a turboprop that runs on Jet A or LH_2, particularly after considering the avoided energy from liquefaction of hydrogen. Revolutionary designs, such as the BWB aircraft, are another area of potential research. These revolutionary designs could provide additional efficiencies and larger fuselage volumes that could enhance the addressable market of LH_2-powered aircraft.

Finally, additional research is needed on the non-CO_2 climate impact of fossil jet fuel, and the potential for hydrogen to abate the impact of contrail cirrus. This co-benefit could distinguish hydrogen from other aviation fuels and justify additional policy support, for example by integrating non-CO_2 climate abatement into carbon pricing or alternative fuel mandates.

Even after considering the performance penalties for carrying LH_2 as a fuel source, the aircraft modeled in this work can capture a large section of the aviation market. They can provide significant reductions in carbon emissions of the captured market but can, at a maximum, cap global passenger aviation emissions at 2035 levels. The aircraft can fit into existing airline route operations but will require significant investment in infrastructure to make them viable.

BIBLIOGRAPHY

Air Transport Action Group (ATAG). (2011). *Powering the future of flight*. ATAG. https://seors.unfccc.int/applications/seors/attachments/get_attachment?code=GRPR31ZA287D3KAP5XOXQO2WP1JE9SQQ

Air Transport Action Group (ATAG). (2021, October 5). *Aviation Industry Adopts 2050 Net-Zero Carbon Goal*. https://www.atag.org/our-news/press-releases.html?view=pressrelease&id=125

Airbus. (n.d.). *A320neo*. Airbus. Retrieved September 28, 2021, from https://www.airbus.com/aircraft/passenger-aircraft/a320-family/a320neo.html

Airbus. (2020, September 20). *ZEROe*. Airbus. https://www.airbus.com/innovation/zero-emission/hydrogen/zeroe.html

Aircraft – Eviation. (n.d.). Retrieved November 12, 2021, from https://www.eviation.co/aircraft/

Argonne National Laboratory. (2020). *The Greenhouse gases, Regulated Emissions, and Energy use in Transportation Model (GREET)* (Version 2020) [Computer software]. https://greet.es.anl.gov/index.php

ATR. (2020, July 10). *ATR 72-600 Aircraft | ATR Aircraft*. ATR. https://www.atr-aircraft.com/our-aircraft/atr-72-600/

Botero, E. M., Wendorff, A., MacDonald, T., Variyar, A., Vegh, J. M., Lukaczyk, T. W., Alonso, J. J., Orra, T. H., & Ilario da Silva, C. (2016, January 4). SUAVE: An Open-Source Environment for Conceptual Vehicle Design and Optimization. *54th AIAA Aerospace Sciences Meeting*. 54th AIAA Aerospace Sciences Meeting, San Diego, California, USA. https://doi.org/10/gm3hdx

Brownley, J. (2021, February 4). *Text - H.R.741 - 117th Congress (2021-2022): Sustainable Aviation Fuel Act* (2021/2022) [Legislation]. https://www.congress.gov/bill/117th-congress/house-bill/741/text

Brynolf, S., Taljegard, M., Grahn, M., & Hannsson, J. (2018). Electrofuels for the transport sector: A review of production costs. *Renewable and Sustainable Energy Reviews*, *81*, 1887–1905. https://doi.org/10/gcrpxh

California Air Resources Board. (2021, October 21). *Dashboard | California Air Resources Board*. Dashboard | California Air Resources Board. https://ww3.arb.ca.gov/fuels/lcfs/dashboard/dashboard.htm

Chevron. (2007). *Aviation Fuels Technical Review*. Chevron. https://www.chevron.com/-/media/chevron/operations/documents/aviation-tech-review.pdf

Embraer. (2021). *Energia Hybrid E9-HE Spec Sheet*. https://embraercommercialaviationsustainability.com/wp-content/uploads/2021/11/Spec-Energia-Hybrid.pdf

European Commission. (2021a). *Regulation of the European Parliament and of the Council on ensuring a level playing field for sustainable air transport*. https://ec.europa.eu/info/sites/default/files/refueleu_aviation_-_sustainable_aviation_fuels.pdf

European Commission. (2021b). *Proposal for a Regulation of the European Parliament and of the Council on ensuring a level playing field for sustainable air transport* (COM(2021) 561 final-2021/0205 (COD)). https://ec.europa.eu/info/sites/default/files/refueleu_aviation_-_sustainable_aviation_fuels.pdf

European Commission. Joint Research Centre. (2020). *Fossil CO_2 and GHG emissions of all world countries: 2020 report.* Publications Office. https://data.europa.eu/doi/10.2760/143674

Federal Aviation Administration (FAA). (2021). *2021 United States Aviation Climate Action Plan* (p. 40). Federal Aviation Agency. https://www.faa.gov/sites/faa.gov/files/2021-11/Aviation_Climate_Action_Plan.pdf

Gomez, A., & Smith, H. (2019). Liquid hydrogen fuel tanks for commercial aviation: Structural sizing and stress analysis. *Aerospace Science and Technology*, *95*, 105438. https://doi.org/10.1016/j.ast.2019.105438

Graver, B., & Rutherford, D. (2018). *U.S. Passenger Jets under ICAO's CO_2 Standard, 2018-2038*. International Council on Clean Transportation. https://theicct.org/publications/us-passenger-jets-icao-co2-standard

Graver, B., & Rutherford, D. (2021). *Low-cost carriers and U.S. aviation emissions growth, 2005 to 2019*.

Graver, B., Rutherford, D., & Zheng, S. (2020). *CO_2 emissions from commercial aviation: 2013, 2018, and 2019*. International Council on Clean Transportation. https://theicct.org/publications/co2-emissions-commercial-aviation-2020

Heart Aerospace | Electrifying regional air travel. (n.d.). Retrieved November 11, 2021, from http://heartaerospace.com/

International Air Transport Association (IATA). (2020). *Waypoint 2050*. https://aviationbenefits.org/media/167187/w2050_full.pdf

International Air Transport Association (IATA). (2021, October 4). *Airline Industry Economic Performance—October 2021—Data tables*. https://www.iata.org/en/iata-repository/publications/economic-reports/airline-industry-economic-performance---october-2021---data-tables/

International Civil Aviation Organization (ICAO). (n.d.). *Post-COVID-19 forecasts scenarios tables. pdf*. Retrieved November 12, 2021, from https://www.icao.int/sustainability/Documents/Post-COVID-19%20forecasts%20scenarios%20tables.pdf

International Civil Aviation Organization (ICAO). (2018). *Annex 16—Environmental Protection, Volume IV, Carbon Offsetting and Reduction Scheme for International Aviation (CORSIA): Vol. IV* (1st ed.). https://www.icao.int/environmental-protection/CORSIA/Pages/SARPs-Annex-16-Volume-IV.aspx

International Civil Aviation Organization (ICAO). (2020). *CORSIA approved sustainability certification schemes*. https://www.icao.int/environmental-protection/CORSIA/Documents/ICAO%20document%2004%20-%20Approved%20SCSs.pdf

International Civil Aviation Organization (ICAO), Council, & International Civil Aviation Organization. (2016). *Aerodromes: International standards and recommended practices. Volume I. Volume I.*

International Energy Agency. (IEA). (2019). *The Future of Hydrogen – Analysis*. IEA. https://www.iea.org/reports/the-future-of-hydrogen

Intergovernmental Panel on Climate Change. (IPCC). (2014). *Climate Change 2014: Synthesis Report. Contribution of Working Groups I, II and III to the Fifth Assessment Report of the Intergovernmental Panel on Climate Change* (p. 151). https://www.ipcc.ch/report/ar5/syr/

Lee, D. S., Fahey, D. W., Skowron, A., Allen, M. R., Burkhardt, U., Chen, Q., Doherty, S. J., Freeman, S., Forster, P. M., Fuglestvedt, J., Gettelman, A., De León, R. R., Lim, L. L., Lund, M. T., Millar, R. J., Owen, B., Penner, J. E., Pitari, G., Prather, M. J., … Wilcox, L. J. (2021). The contribution of global aviation to anthropogenic climate forcing for 2000 to 2018. *Atmospheric Environment*, *244*, 117834. https://doi.org/10.1016/j.atmosenv.2020.117834

Lukaczyk, T. W., Wendorff, A. D., Colonno, M., Economon, T. D., Alonso, J. J., Orra, T. H., & Ilario, C. (2015, June 22). SUAVE: An Open-Source Environment for Multi-Fidelity Conceptual Vehicle Design. *16th AIAA/ISSMO Multidisciplinary Analysis and Optimization Conference*. 16th AIAA/ISSMO Multidisciplinary Analysis and Optimization Conference, Dallas, TX. https://doi.org/10/gm3hdz

Makridis, S. (2016). Hydrogen storage and compression. *ArXiv:1702.06015 [Cond-Mat, Physics:Physics]*, 1–28. https://doi.org/10/gkf96k

McKinsey & Company. (2020). *Hydrogen-powered aviation A fact-based study of hydrogen technology, economics, and climate impact by 2050*. Clean Skys 2 JU. https://www.fch.europa.eu/sites/default/files/FCH%20Docs/20200507_Hydrogen%20Powered%20Aviation%20report_FINAL%20web%20%28ID%208706035%29.pdf

Mikosz, S. (2021, October 4). *Airline commitment to Net Zero 2050*. IATA Annual General Meeting, Boston, MA. https://www.iata.org/en/iata-repository/pressroom/presentations/environment-net-zero-carbon-at-iata-agm-2021/

MIT OCW. (2006, April 6). *Lab 8 Notes—Basic Aircraft Design Rules*. https://ocw.mit.edu/courses/aeronautics-and-astronautics/16-01-unified-engineering-i-ii-iii-iv-fall-2005-spring-2006/systems-labs-06/spl8.pdf

Ponater, M., Pechtl, S., Sausen, R., Schumann, U., & Hüttig, G. (2006). Potential of the cryoplane technology to reduce aircraft climate impact: A state-of-the-art assessment. *Atmospheric Environment*, *40*(36), 6928–6944. https://doi.org/10.1016/j.atmosenv.2006.06.036

Scholz, D. (n.d.). Aircraft Design—Chapter 5 Preliminary Sizing. In *Aircraft Design*. Hamburg Open Online University (HOOU). Retrieved November 12, 2021, from https://www.fzt.haw-hamburg.de/pers/Scholz/HOOU/AircraftDesign_5_PreliminarySizing.pdf

U.S. Energy Information Administration. (2021). *Annual Energy Outlook 2021, Table 12: Petroleum and Other Liquids Prices, Reference case*. https://www.eia.gov/outlooks/aeo/data/browser/#/?id=12-AEO2021&cases=ref2021&sourcekey=0

Verstraete, D. (2009). *The Potential of Liquid Hydrogen for long range aircraft propulsion*. http://dspace.lib.cranfield.ac.uk/handle/1826/4089

Wells, D. P., Horvath, B. L., & McCullers, L. A. (2017). *The Flight Optimization System Weights Estimation Method*. 91.

Welstead, J., & Felder, J. L. (n.d.). Conceptual Design of a Single-Aisle Turboelectric Commercial Transport with Fuselage Boundary Layer Ingestion. In *54th AIAA Aerospace Sciences Meeting*. American Institute of Aeronautics and Astronautics. https://doi.org/10.2514/6.2016-1027

Westenberger, A. (2003). *Liquid Hydrogen Fuelled Aircraft – System Analysis, Final Technical Report (Publishable version)* [Final Technical Report].

Winnefeld, C., Kadyk, T., Bensmann, B., Krewer, U., & Hanke-Rauschenbach, R. (2018). Modelling and Designing Cryogenic Hydrogen Tanks for Future Aircraft Applications. *Energies*, *11*(1), 105. https://doi.org/10/gc6qjm

ZeroAvia | Alaska Air Group | Hydrogen Powertrain. (2021, October 26). ZeroAvia. https://www.zeroavia.com/alaskaair

Zhou, Y., & Searle, S. (Forthcoming). *Current and future cost of e-kerosene in the United States and Europe*. International Council on Clean Transportation.

Zhou, Y., Searle, S., & Baldino, C. (forthcoming). *Cost of Renewable Hydrogen Produced Onsite at Hydrogen Refueling Station in Europe*. The International Council on Clean Transportation.

Zhou, Y., Swidler, D., Searle, S., & Baldino, C. (2021). *Life-cycle greenhouse gas emissions of biomethane and hydrogen pathways in the European Union*. International Council on Clean Transportation. https://theicct.org/publications/lca-biomethane-hydrogen-eu-oct21

APPENDIX A: HYDROGEN STORAGE

While detailed tank design is beyond the scope of this work, existing cryogenic tank design research is leveraged to provide realistic values for the properties of the tank (Gomez & Smith, 2019; Verstraete, 2009; Winnefeld et al., 2018).

Table A1 highlights the fuel storage assumptions used in our modeling. The hydrogen storage is assumed to be a single cylindrical tank that resides behind the rear bulkhead of the passenger cabin. The tank is assumed to be integral to the fuselage, i.e., the tank must be able to handle the loads exerted on the fuselage. The volume utilization of 92.7% refers to the percentage of the available fuselage volume that can be filled by the liquid hydrogen. This considers the thickness of the tank's structural and thermal layers. The fill pressure is set to be higher than atmospheric pressure to ensure air cannot enter the tank.

Table A1. Liquid hydrogen storage properties

Property	Value
Volume utilization (η_v)	92.7%
Fill pressure	1.2 bar
Venting pressure	3.5 bar
Maximum fill percentage (η_f)	85%
Gravimetric index (*GI*)	0.2 – 0.35

Even with high-quality thermal insulation from the ambient environment, small amounts of heat will inevitably penetrate the tank into the stored LH_2. This causes some of the LH_2 to vaporize into GH_2. This phenomenon, referred to as boil-off, increases the pressure in the tank. If the pressure increases beyond the tank's stated venting pressure, the GH_2 must be vented out into the atmosphere to avoid tank failure. Venting hydrogen is costly and needs to be avoided. For this reason, the tanks are designed with a venting pressure of 3.5 bar. This is high enough to withstand the amount of boil-off that is expected over the duration of an aircraft's mission, without needing to vent and waste the GH_2 (Ponater et al., 2006).

The combination of the fill pressure, the venting pressure, and the need to have a minimum volume of GH_2 at the venting pressure limits the maximum allowable fill percentage of the tank to 88.5% (Verstraete, 2009). With an additional 3.5% of volume allowance for internal baffles, tank shrinkage, and unusable fuel, the maximum usable fill percentage (η_f) is further limited to 85%. This results in a maximum volume of LH_2 carried by an aircraft to

$$V_{LH2} = \eta_f \eta_V \pi R_{fuse}^2 L_{tank},$$

where R_{fuse} is the radius of the fuselage and L_{tank} is the length of the fuel tank. The R_{fuse} is kept the same as the reference aircraft. This leaves the L_{tank} as the only independent variable that is used to change the volume of LH_2 carried. However, with the fuselage length limits on the design dictated by feasibility constraints, the L_{tank} is often set to the maximum value that would maximize the allowable fuselage length.

The volume of LH_2 and its density is used to derive the mass of LH_2 that is carried by the aircraft. The gravimetric index is then used to calculate the mass of the fuel system. This is added to the Operating Empty Weight (OEW) of the aircraft as determined by the weight estimation module.

Throughout this work we have mentioned the importance of LH_2 storage technology in the performance metrics of these aircraft and have presented results with GI values of 0.2 and 0.35. The high end of the range, GI = 0.35, would achieve specific energy parity between hydrogen and Jet A. With aircraft configurations defined and the addressable

market quantified, we sweep gravimetric index values to see how it changes the RPK coverage and the MTOM of the aircraft. The results are shown in Figure A1 and Figure A2 for the turboprop and the narrow-body aircraft, respectively. For the family of aircraft, the MTOM is the average across the three configurations.

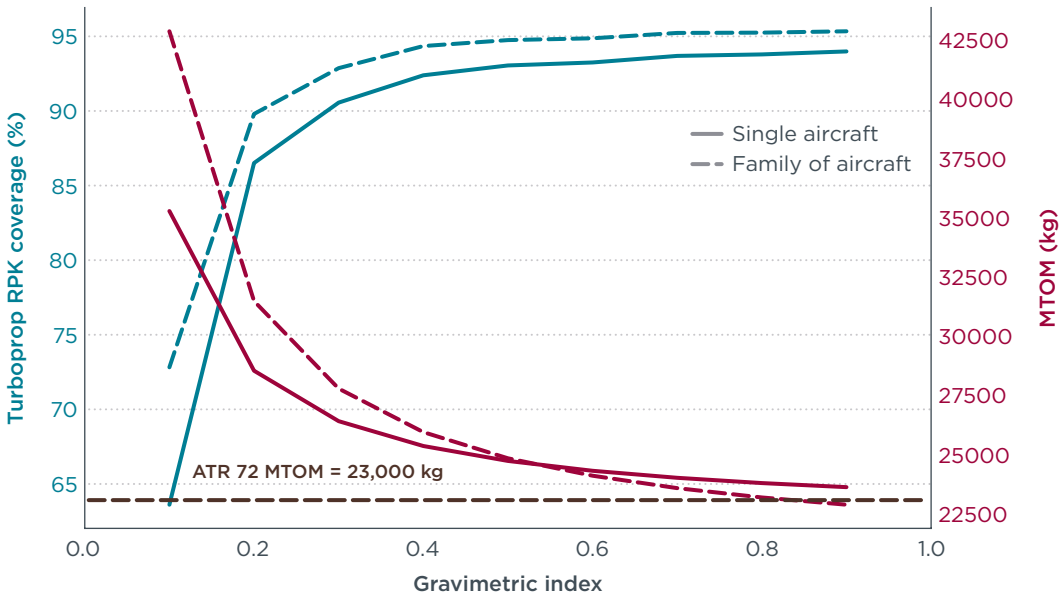

Figure A1. Turboprop RPK coverage and MTOM as a function of the LH_2 fuel system's gravimetric index.

Similar trends are seen across the different cases. As the gravimetric index increases, MTOM drops but asymptotically approaches a minimum weight depending on the structure and payload of the aircraft. The RPK coverage increases, but also asymptotically reaches a maximum. Huge improvements in coverage are seen up to GI of 0.35, at which point the LH_2 system stops paying a mass penalty. Beyond that point, the performance is limited by the volumetric storage of LH_2. This is because changing the gravimetric index only changes the weight of the tank; it does not change the tank's size, which is constrained by the maximum allowable fuselage length. A higher fidelity analysis could justify changes to existing aircraft geometry to support a larger fuel tank based upon this lower MTOM but is beyond the scope of this work.

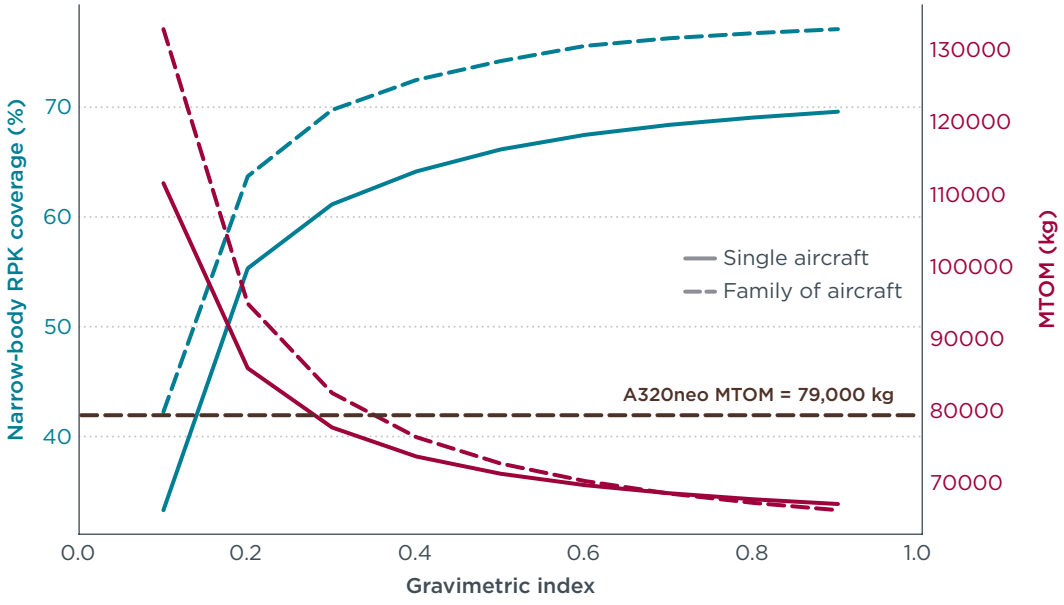

Figure A2. Narrow-body RPK coverage and MTOM as a function of the LH_2 fuel system's gravimetric index.

APPENDIX B: AIRCRAFT MISSION PROFILE

The aircraft missions are defined by a sequence of climb, cruise, and descent segments. We use Piano 5's default mission for the reference aircraft as a template. Accordingly, the turboprop mission segments are:

1. Climb to 1,500 feet at a constant Calibrated Airspeed (CAS) of 64 m/s and a climb rate of 1650 ft/min
2. Climb to 10,000 feet at a constant CAS of 75 m/s and a climb rate of 1330 ft/min
3. Climb to 20,000 feet at a constant CAS of 75 m/s and a climb rate of 1000 ft/min
4. Cruise at 20,000 feet at Mach 0.452
5. Descent to 10,000 feet at a constant CAS of 100 m/s and a descent rate of 1060 ft/min
6. Descent to 1,500 feet at a constant CAS of 100 m/s and a descent rate of 1020 m/s
7. Descent to 35 feet at a constant speed of 55 m/s and a descent angle of 3°

The narrow-body turbofan mission segments are:

1. Climb to 1,500 feet at a constant CAS of 90 m/s and a climb rate of 2450 ft/min
2. Climb to 10,000 feet at a constant CAS of 129 m/s and a climb rate of 2800 ft/min
3. Climb to 30,000 feet starting at Mach 0.42 to Mach 0.71 at a climb rate of 1800 ft/min
4. Climb to 35,000 feet at a constant Mach of 0.717 and a climb rate of 1300 ft/min
5. Cruise at 35,000 feet at Mach 0.78
6. Descent to 30,000 feet at a constant Mach of 0.717 and a descent rate of 2,400 ft/min
7. Descent to 10,000 feet at a constant CAS of 137.7 m/s and a descent rate of 2,000 ft/min
8. Descent to 1,500 feet at a constant CAS of 129 m/s and a descent rate of 1,500 ft/min
9. Descent to 35 feet at a constant speed of 68 m/s and a descent angle of 3°

For simplicity and direct aircraft performance comparisons, step-up cruise segments are not used. The cruise segments for both aircraft are at a constant altitude and constant Mach number.

The following fuel reserves are included when determining aircraft range:

1. Flight to an alternate airport 185 km (100 nautical miles) away.
2. 45 minutes of loitering above the airport.
3. 5% of the block fuel as contingency.

In addition to running simulations to determine the maximum range of the aircraft, we run missions that are representative of current routes flown by the reference aircraft. We collect all routes flown by the aircraft in 2019 (Graver et al., 2020) and determine the median and 90th percentile route lengths. In the case of the ATR 72, 50% of the missions were < 400 km long, and 90% of the missions were < 750 km long. For the A320neo 50% of the missions were < 1,500 km and 90% of the missions were < 3,180 km long.